Master's thesis

2022

Jakob Anglevik

NTNU
Norwegian University of
Science and Technology
Faculty of Natural Sciences
Department of Chemical Engineering

Jakob Anglevik

CO_2 absorption from industrial clusters

June 2022

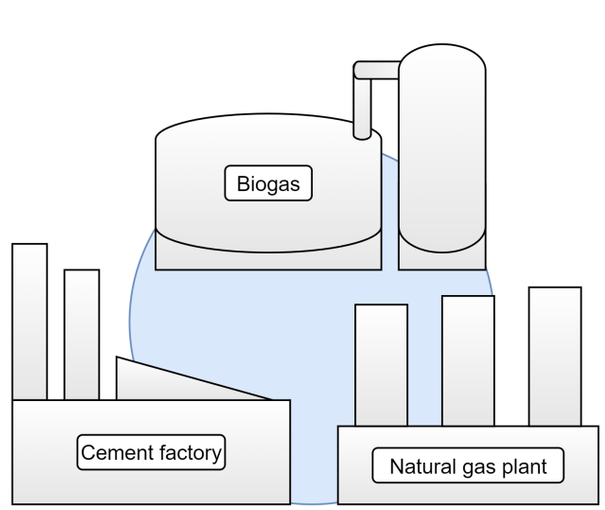

NTNU
Norwegian University of
Science and Technology

NTNU
Norwegian University of
Science and Technology

NTNU
Norwegian University of
Science and Technology

CO_2 absorption from industrial clusters

Jakob Anglevik

Chemical engineering
Submission date: June 2022
Supervisor: Hanna Knuutila
Co-supervisor: Andressa Nakao

Norwegian University of Science and Technology
Department of Chemical Engineering

TKP4900 Kjemisk prosessteknologi, masteroppgave

Department of Chemical engineering

CO_2 absorption from industrial clusters

Author
Jakob Anglevik

Supervisors
Hanna Knuutila and Andressa Nakao

June 20, 2022

NTNU

Abstract

This thesis has used Aspen plus to simulate different capture cluster configurations to find the most efficient way to capture CO_2 from multiple emission sources using amine absorption. This has been done by examining 3 different CO_2 cluster configurations for capturing CO_2 from a natural gas power plant, a cement plant, and a biogas plant at different scales. The first configuration is represented as the base case, where each plant is equipped with an absorber and a stripper. Totaling 3 absorbers, 3 strippers for 3 plants. The second configuration uses 3 absorbers and 1 stripper, called the 3-1 cluster. In this scenario the solvent from each absorber is to be pumped to the stripper to be regenerated and pumped back to the absorber. The third configuration would look at using 1 absorber and stripper, called 1-1 cluster. The flue gas from the nearby plants would be pumped to this central absorber and stripper.

To quantify the cost of the different capture configurations, amine absorption has been simulated in Aspen plus. This data has been used to calculate the capital cost, running cost of each facility, and the price for all the different pumping options. The findings of this work are that significant savings can be made by using the 3-1 cluster configurations. An example case shows that for a large industry scale biogas, cement and natural gas plant the capital cost can be lowered from 610 to 532 $ MM, and the running cost for the capture facilities can be lowered from 96 to 85 $ MM. for the 1-1 cluster there are potential savings, but these drop off quickly with increasing distance between the plants.

Sammendrag

Denne oppgaven har brukt Aspen plus til å simulere forskjellige konfigurasjoner for CO_2 fangst, for å finne den mest effektive måten å fange CO_2 fra flere utslippskilder ved å bruke aminabsorpsjon. Dette er gjort ved å undersøke 3 forskjellige CO_2-klynge konfigurasjoner for fangst av CO_2 fra et naturgasskraftverk, et sementanlegg og et biogassanlegg i ulike skalaer. I den første konfigurasjonen er hvert anlegg er utstyrt med en egen absorber og en stripper. Totalt 3 absorbere, 3 strippere for 3 anlegg. Den andre konfigurasjonen bruker 3 absorbere og 1 stripper, kalt 3-1 klyngen. I dette scenariet skal aminløsningen fra hver absorber pumpes til stripperen for å bli regenerert og pumpes tilbake til absorberen. Den tredje konfigurasjonen ville se på å bruke 1 absorber og 1 stripper, kalt 1-1 klynge. Røykgassen fra de nærliggende anleggene skulle pumpes til denne sentrale absorberen og stripperen.

For å kvantifisere kostnadene for de forskjellige fangstkonfigurasjonene, er aminabsorpsjon blitt simulert i Aspen plus. Disse dataene har blitt brukt til å beregne kapitalkostnaden, driftskostnaden for hvert anlegg og prisen for alle de forskjellige pumpealternativene. Funnene av dette arbeidet er at betydelige besparelser kan gjøres ved å bruke 3-1 klyngekonfigurasjoner. Et eksempel viser at for et biogass-, sement- og naturgassanlegg i stor industriskala kan kapitalkostnaden reduseres fra 610 til 532 $ MM, og driftskostnaden for fangstanleggene kan senkes fra 96 til 85 $ MM. For 1-1 klyngen er det potensielle besparinger, men disse faller fort bort ved en lang distanse mellom utslippskilden og absorberen.

Contents

List of Figures

List of Tables

1 Introduction

Global warming is one of the biggest challenges humanity face in the 21 Th century [1]. By emitting increasingly amounts of CO_2 into the atmosphere, the global temperature of the world has already increased by 1 °C since pre-industrial eras [2]. The increase in temperature poses a great threat to many climates across the globe, and higher temperatures leads to increased frequency and severity of natural disasters such as flooding, droughts and hurricanes [3]. The Intergovernmental Panel on Climate Change (IPCC) has stated that to avoid climate disaster the rise in global temperature should be kept as low as possible. To be able to reach the goal of stopping the global warming at 1.5 or even 2.5 °C, IPCC and The international energy agency has stated that Carbon capture has to play a vital role [4] [5].

In order to capture CO_2 from industrial plants, there exist several technology principles, such as membrane separation, adsorption, chemical looping and absorption. For CO_2 capture, amine absorption is the most mature technology, with several operational pilot plants running today [6] [7] [8] [9]. Amine absorption works by scrubbing the CO_2 rich gas in absorber, where the co2 is absorbed in the liquid used in the absorber. The liquid is then pumped to a stripper where the CO2 is stripped from the liquid solvent. The large challenges facing amine absorption are the large investment costs for constructing capture facilities, and a high energy requirement for CO_2 per ton captured [10] [11].

One way to mitigate the issue of high investment cost, would be if several CO_2 emitting plants could be connected to the same capture facility in an industrial cluster.This can be done by pumping the flue or product gas containing CO_2 from the source to one big capture facility. Another configuration would be to have absorbers at each CO_2 source, and pump the CO_2 rich liquid to one large stripper which would strip solvents from several absorbers. The CO_2 sources would have to be reasonably close to each other, examples of this is an oil refinery, where there are multiple facilities producing CO_2 [12]. Today there is very few or no studies comparing or quantifying the different configurations of capture. This thesis aims to quantify the differences between the different capture configurations by: sizing the equipment, finding the total investment costs, and running costs, and power usage for the different configurations.

This is done by simulating the different plant configurations in Aspen plus, and using cost estimation methods from Sinnott and Towler's chemical engineering and design.

Industrial plants have a range of CO_2 concentrations and volumes of flue gas from different processes. To see how this would impact the capture conditions plants with very varying CO_2 streams are investigated. natural gas power plants has high gas volume but low concentrations, biogas upgrading plants process a low amount of gas but

has a very high concentration of CO_2. Cement plants provide a middle ground between these two.

1.1 Outline of thesis

The background and theory chapter goes explain how CO_2 is formed in the different plants investigated in this thesis. An overview of amine absorption related to carbon capture is presented with theory of mass transfer. The theory for the cost calculation are detailed and how the sizing has been done for all the major equipment. The thesis will detail how the cost of different pipelines are found.

In chapter 3 model validation, experimental vapour liquid equilibrium are assessed against values from Aspen plus to give an estimate on accuracy of the simulation. The absorber and stripper are validated against pilot plants to quantify the expected errors in the simulations.

The method is presented in chapter 4, which gives insight into the the sizes and configurations of the different capture facilities. it details how most of the design choices were made in simulating the different cases.

Chapter 5 is the results chapter which goes into detail on the results for the medium sized cement CO_2 capture plant, a summary of the overall results, and shows sensitivity analysis done for the plants. An example of capture configurations is shown in the end of the results to get a better overview of the results presented.

Chapter 6 contains the conclusions from this thesis.

2 Backgorund and theory

To reduce anthropogenic CO_2 emissions Carbon capture and storage (CCS) can be utilised. The main objective of CCS is to separate of CO_2 from a gas mixture and produce a pure CO_2 gas that can be stored. The gas mixture from which the CO_2 is separated from vary depending on how the CO_2 is produced. The different ways CO_2 is produced is explained below.

2.1 Cement production

Cement production is responsible fro aproximatley 5% of anthrophogenic CO_2 emissions[13]. The most CO_2 intensive part of cement production is the manufacturing of the cement clinker[14], which is the main component of modern cement. In this step 60% of the CO_2 comes from the calcination reaction of limestone ($CaCO_3$) , while the other 40% comes from the combustion of fossil fuels to heat the furnace to drive the reaction. In the calcination reaction, ($CaCO_3$) is burned in a kiln to produce calcium oxide and CO_2 through reaction 2.1.

$$CaCO_3(s) \rightarrow CaO(s) + CO_2(g) \tag{2.1}$$

This reaction is responsible for the high CO_2 concentration (16-30 %)[13] of the flue gas from the cement plants, since the CO_2 produced from the reaction is mixed with the CO_2 from the furnace heating the reaction.

2.2 Biogas

Biogas is made from the anaerobic breakdown of protein, fats and carbohydrates, which can come from a range of organic matter. The feed sources includes sewage sludge, livestock manure, household organic waste, and energy crops. The reaction steps in a bioreactor is hydrolysis, acidogenesis, acetogenesis, and methanogenesis to create Methane(CH_4) and CO_2. The compostion of the biogas will differ based on the feedstock used, and the reactor conditions. It is composed of 50–75 % methane, 25–50 % carbon dioxide, 0–10 % nitrogen, 0–3 % hydrogen sulfide[15].

2.3 Combustion of fossil fuels

As of 2020, 63% of the worlds electricity is produced by combustion of fossil fuels[16]. Coal and natural gas are the main combustibles used for electricity production, and they produce heat and CO_2 through reaction 2.2 and 2.3 respectively. The heat of the reaction is utilised by either powering a gas turbine and or heating steam to a steam

turbine.

$$\mathrm{C} + \mathrm{O}_2 \rightarrow \mathrm{CO}_3 \tag{2.2}$$

$$C_n H_{2n+2} + \mathrm{O}_2 \rightarrow n\mathrm{CO}_2 + 2n\mathrm{H}_2\mathrm{O} \tag{2.3}$$

2.4 Amine absorption

Amine absorption was first patented in 1930 as a method to remove H_2S and[9]. Today it is the leading choice for post combustion CO_2 capture[9]. Amine absorption works by contacting a CO_2 rich gas with an aqueous amine solvent. The solvent will react with the CO_2 to form carbonates and carbamates. The solvent can then later be heated up, to release the CO_2 in gas form. In practise this is done with an absorber and stripper, which is depicted in the simplified process flow sheet 2.1.

The gas enter the bottom of the absorber and travels upward, while the liquid solvent enters the top. The absorber is designed to have a high contact area between the gas and liquid, to facilitate as much mass transfer ass possible, this is done either by filling the absorber column with packing materiel, or with trays. As the liquid solvent travels down the absorber it absorbs CO_2 until the bottom were the solvent is filled with CO_2. The amount of CO_2 a solvent contains is measured in loading of the solvent which is molar concentration of CO_2 divided by the molar concentration of MEA. The solvent exists the the bottom of the absorber with a higher loading than entering, and is in its rich state. The solvent has a high affinity to absorb CO_2 when it is in its cold state, and low affinity as the solvent is heated. This principle is used to regenerate the rich solvent. It is heated in a Stripper column, and the solvent will lose a fraction of its CO_2. The stripper will have nearly pure CO_2 as a product, and the solvent will exit with a low loading, ready to be used again in the absorber once it's cooled.

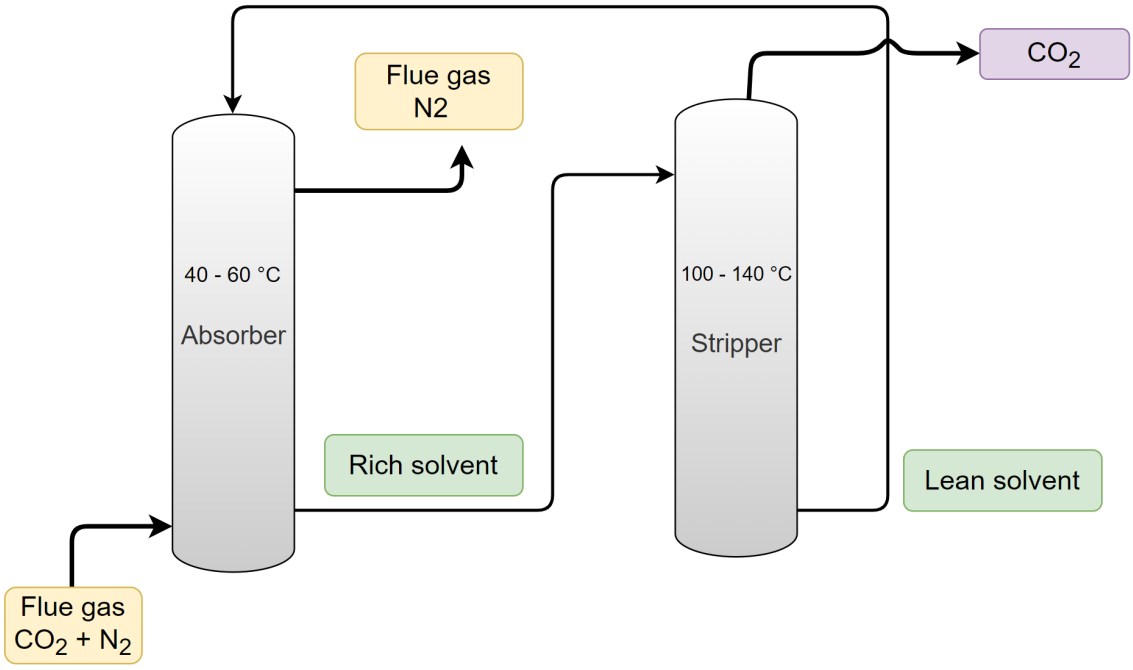

Figure 2.1: A simplified flow sheet of CO_2 absorption using amine absorption

2.4.1 Mass transfer of absorption

The driving force behind the absorption of CO_2 is the difference in the partial pressure of CO_2 and the concentration of dissolved CO_2 in the liquid at equilibrium, described in equation 2.4. The concentration of CO_2 in the liquid at equilibrium is described by henry's law in equation 2.5.

$$\text{Driving force} = P_{CO_2} - P^*_{CO_2} \tag{2.4}$$

$$C^* = k \cdot P^*_{gas} \tag{2.5}$$

C is the concentration of the gas species in the liquid at equilibrium. k is the henry constant for the gas. P^*_{gas} is the partial pressure of the gas at equilibrium.

One of the models used to describe mass transfer between two phases, is the film theory. The film theory is based on the idea that a fluid film forms where there is contact between two phases. In this film the mass transfer is only through diffusion and all the overall resistance to mass transfer is in this film. How fast the absorption happens is then dependent on the overall mass transfer coefficient K_G and the thickness of this film. For CO_2 absorption this rate coefficient is described by combining the diffusion coefficient of CO_2 in the liquid, and the enhancement factor E as in equation 2.6. Mass transfer resistance in the gas phase is disregarded as it is magnitudes lower than resistance in the liquid phase. The enhancement factor is to account for the chemical reactions taking place in the liquid, speeding up mass transfer. The diffusion coefficient is found by equation 2.7.

$$\frac{1}{K_{\mathrm{G}}} = \frac{1}{k_{\mathrm{L}} \cdot \mathrm{E}} \tag{2.6}$$

$$k^*_{\mathrm{L}} = \frac{D_{\mathrm{CO_2,L}}}{\delta_{\mathrm{L}} h_{\mathrm{CO_2,L}}} \tag{2.7}$$

$D_{CO_2(L)}$ is the Diffusion coefficient of the gas in the liquid phase . $\delta_(L)$ is the thickness of the stagnant film on the liquid side.

The rate of mass transfer N_{CO_2} $[mol/(m^2 s]$ is given by the driving force and overall mass transfer coefficient shown in equation 2.8.

$$N_{CO_2} = K_G \left(P_{CO_2} - P^*_{CO_2} \right) \tag{2.8}$$

The mass transfer across the films using film theory is described by figure 2.2.

2.2.

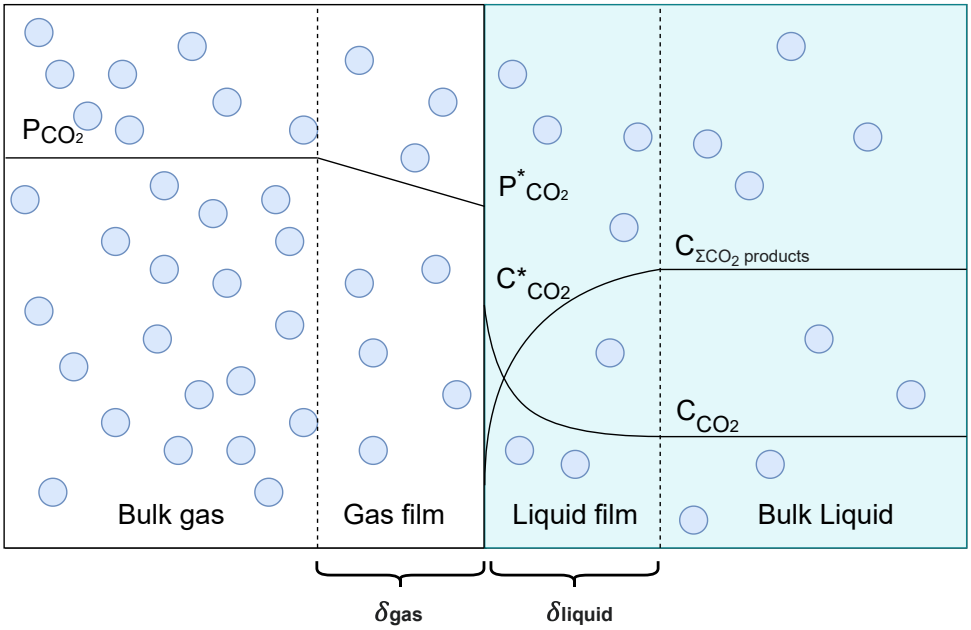

Figure 2.2: Film theory describing mass transfer for CO_2 absorption

2.5 Monoethanolamine

Monoethanolamine (MEA) is one of the most widely used amines for sour gas scrubbing and co2 capture[17]. The advantages of MEA is that it is relatively cheap to produce, it is a primary amine with an excellent acid dissociation constant, which gives it an above average normalized capacity and good rate of absorption. The heat of absorption is high resulting in good performance in thermal swing regeneration. The downsides of MEA is that it is prone to oxidative degradation, and at temperatures above 120 °C thermal degradation is rapid[18].

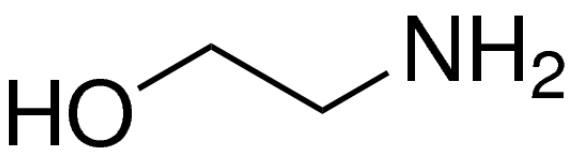

Figure 2.3: structure formula of monoethanolamine

As MEA is a reactive amine, the main mechanism for CO_2 absorption is the formation of carbamate. however, the reaction pathways for the absorption is highly disputed, and there are different mechanisms proposed for different loadings and different partial pressures of CO_2 [19].

2.6 Cost Calculation

To estimate the cost of the different plants examined in this thesis, Sinnot and Towlers (S&T) fixed capital investment estimation from the book Chemical engineering design will be used [20]. The cost estimate for this thesis in in the class 4 for feasibility study, which is used to make choice on design alternatives. This means the accuracy should be around ± 30 %. In this book they present methods for estimating the purchased cost for all the major equipment in the plant, and correlations and factors to further estimate the entire capital investment necessary from the purchase cost of the equipment.

The Fixed capital cost is divided into:

- The inside battery limits (ISBL) costs are costs of the plant itself.
- Off-site battery limit (OSBL) investment includes the cost of improving the site infrastructure to accommodate an industrial plant. This will often include interactions with utility companies to provide Electric main substations, water pipes and site draining etc.
- Engineering and construction costs for design of the plant.
- Contingency charges, which accounts for unexpected costs encountered in the project. This sum will vary depending on how novel or mature the plant technology is.

2.7 Sizing major equipment

The first step in finding the cost is to size all major equipment in the plant. For the amine absorption this will include the absorber, stripper, water wash, pumps, heat exchangers fans and compressors. The units used for sizing this equipment is either the mass of the shell for vessels, the volume flow, power used by the equipment or heat transfer area. All of these parameters are either directly or indirectly supplied from the Aspen plus simulations. The purchase cost is then found with equation 2.9.

$$C_e = a + bS^n \tag{2.9}$$

C_e = Purchased equipment cost

a, b = Cost constants

S = Size parameter

n = Exponent for the type of equipment

All of the cost constants are given for each equipment depending on equipment type and material. All of the size parameters used in this work is in table 2.1.

Table 2.1: Size paramter and cost facotrs given by Sinnot & Towler for equipment purchased cost.

Equpiment	**Sizing unit**	**Valid sone**		Cost factors		
		Lower size	Upper size	a	b	n
Pressure vessel	Shell mass $[KG]$	120	250,000	50,000	11,000	0.85
Pump	Flow $[L/s]$	0.2	126	6,900	206	0.90
Blower	Flow $[M^3/h]$	200	5,000	3,800	49	0.80
Compressor	Driver power $[kW]$	75	30,000	490,000	16,800	0.60
Heat exchanger	Area $[m^2]$	10	1000	24000	46	1.2
Reboiler	Area $[m^2]$	10	500	25000	340	0.9

2.7.1 Sizing of absorber

The size parameter for the absorber, stripper and water wash is shell mass. Shell mass m can be calculated from equation 2.10 from S & T. Selecting the diameter and height of the absorber is discussed in chapter 4.5.1.

$$m = \pi D_c L_c t_w \rho_m \tag{2.10}$$

D_c = Vessel diameter [m]

L_c = vessel length [m]

t_w = wall thickness [m]

ρ_m = metal density, [kg/m3] 304 Stainless steel 8000 kg/m3

The wall thickness can be calculated from equation 2.11 by S&T [20].

$$t_w = \frac{P_i D_i}{2SE - P_i} \tag{2.11}$$

where:

P_i = Internal pressure [Pa]

D_i = internal diameter (assumed to be the same as D_c) [m]

S = maximum allowable stress [N/m2]

E = Welded-joint efficiency, assumed to be 1.

The maximum allowable stress for stainless steel operating up 140 °C is 15.0 Ksi (103 N/mm2) [21].

2.7.2 sizing of heat exchanger

The size parameter for the heat exchanger is heat transfer area, which can be calculated from equation 2.12. The overall heat-transfer coefficient U will vary depending on what fluid is either side of the exchanger. The values used for U are from Ali et al.[22] and are tabulated in table 2.12. The transferred heat is provided by the Aspen plus simulations

$$A = \frac{Q}{U\Delta T_m} \tag{2.12}$$

Where:

Q = Transferred heat [W]

U = The overall heat-transfer coefficient [U/m2 C]

ΔT_m = The logarithmic mean temperature difference

ΔT_m is calculated by equation 2.13

$$\Delta T_m = \frac{\Delta T_1 - \Delta T_2}{ln\frac{\Delta T_1}{\Delta T_2}} \tag{2.13}$$

Where

ΔT_1 is the temperature difference between hot and cold fluids at one end of the heat exchanger

ΔT_2 is the temperature difference between hot and cold fluids at the other end of the heat exchanger

2.7.3 Total capital cost

To relate the purchased equipment cost to the ISBL, several factors have been proposed to get an accurate estimate of the ISBL. Lang proposed summing up the cost of all the

Table 2.2: Overall heat transfer coefficients for heat exchangers

Exchanger	U [W/m2 C]	Hot side	Colde side
Lean and rich solvent	500	MEA solvent	MEA solvent
Lean solvent cooler	800	MEA solvent	Water
Reboiler	800	Low pressure steam	MEA solvent
Condenser	1000	MEA solvent	water

equipment, and multiplying the sum with a factor shown in equation 2.14, with the factor depending on whether the plant processed fluids, solids or both [23].

$$C = F \cdot \sum C_e \tag{2.14}$$

where:

C = total plant ISBL capital cost;

$\sum Ce$ = total delivered cost of all the major equipment items: reactors, tanks, columns, heat exchangers, furnaces, etc.

F = an installation factor, known as a Lang factor.

F = 3.1 for a solids processing plant

F = 4.74 for a fluid processing plant

F = 3.63 for a fluid and solids processing plant

Hand proposed his factor in 1958 that would use a different factor for each equipment type, which would give a a better estimate for the ISBL. The installation factors proposed by hand used in this thesis is listed in table 2.3 [20].

Table 2.3: Installation factors proposed by Hand used for the equipment in amine absorption

Equpiment type	Installation factor
Compressor	2.5
Heat ecxhanger	3.5
pressure vessels	4
pumps	4
miscelaneous	2.5

Sinnot and Towler present their own factorial method, which is based on many later

works after Lang and Hands factors[20]. They divide the factors based on whether the equipment handles solids, fluids or both. Another factor f_m is introduced, this factor takes into account whether carbon steel or an exotic metal is used. This could give a more detailed estimate for a plant using MEA, as it is corrosive and stainless steel is necessary for all equipment in contact with the solvent. This is already factored in with the pressure vessels, the absorber stripper and water wash, however the higher material cost is not accounted for directly using the other factors.

$$f_m = \frac{\text{purchased cost of item in exotic material}}{\text{purchased cost of item in carbon steel}}$$

The full equation for the ISBL cost is in equation 2.15.

$$C = \sum_{i=1}^{i=M} C_{e,i,CS} \left[(1 + f_p) f_m + (f_{er} + f_{el} + f_i + f_c + f_s + f_l) \right] \tag{2.15}$$

Where:

$M =$ total number of pieces of equipment

$f_p =$ installation factor for piping

$f_{er} =$ installation factor for equipment erection

$f_{el} =$ installation factor for electrical work

$f_i =$ installation factor for instrumentation and process control

$f_c =$ installation factor for civil engineering work

$f_s =$ installation factor for structures and buildings

$f_l =$ installation factor for lagging, insulation, or paint

The factors for a fluid processing plant is given in table 2.4.

After the ISBL has been estimated, this can be used to estimate the OSBL, engineering and contingency costs based on factors. The OSBL costs are usually between 20-50% of the ISBL costs. For petrochemical plants and 30% is suggested as a good estimate if nothing is known about the plant location so this was used here. The Engineering costs are set as 30% of the ISBL and OSBL costs. The contingency charges vary is at least 10 % of the ISBL and OSBL costs. Amine absorption is a mature technology, but there is

Table 2.4: Sinnot & Towler factors for ISBL estimation

Item	Factor
f_p Piping	0.8
f_{er} Equipment erection	0.3
f_{el} Electrical	0.2
f_i Instrumentation and control	0.3
f_c Civil	0.3
f_s Structures and buildings	0.2
f_l Lagging and paint	0.1
f_m Carbon steel	1.0
f_m stainless steel 304/316	1.3

still uncertainties related to solvent behavior in contact with different gases, therefore a contingency of 20 % is used. Using the formula provided by S&T the total fixed capital cost (C_{FC}) is given by equation 2.16.

$$C_{FC} = C \cdot (1 + OSBL) \cdot (1 + D\&E + X) \tag{2.16}$$

Where:

$OSBL$: Outside batter limit = 0.3

$D\&E$: Design and engineering = 0.3

X : Contingency = 0.2

Once the C_{FC} has been found, the running costs and income will be found for the plant. To assess the economic viabilty, a simpe pay back time will be used 2.17. This means disregarding any added cost by cost of captial, depriiciation, taxes. This is due to the cases presented in this thesis being generic, and the simple pay back time is the best measurement of economic viability at this stage.

$$\text{Simple pay-back time} = \frac{\text{Total investment}}{\text{Average annual cash flow}} \tag{2.17}$$

2.8 Variable cost of production

These running costs are dependent on how often the plant operates throughout the year. The running costs include the electricity used for all major equipment, the price of steam for the reboiler and replacing lost MEA. These costs are tabulated in table 2.5.

Table 2.5: Prices used for cost calculation

Cost	Price	Reference
Electricity price	0.08 $/kwH	A [24]
Steam price	17 $/ton	B [22]
MEA price	1866 $/m3	B [22]
Cost year and currency	USD 2022	

2.8.1 Price of electricity

Electricity price varies a lot from country to country, and with resent European sanctions and worsening relation towards Russia worsening the electricity price is hard to predict [25]. As recent prices for power have been highly variable, the 2019 EU average of 0.08 $/kWh was chosen to select a price from when prices were more stable [24].

2.8.2 Price of steam

The biggest single cost of production is the heat to the reboiler. Aspen plus provides the reboiler duty, and this has to be calculated to a running cost. Several authors use different methods for equating reboiler duty to running costs. Ali et al. uses the price per ton of steam [22], while some such as Nwoaha et al. [26] use a set price based on per GJ the reboiler uses, while Aromada use the reboiler duty and calculate the cost as 25% of electricity cost [27]. In this thesis LP with a heating value of 2.1 MJ/kg was used and the price was calculated based on tonnes steam necessary. To find the cost of the steam in the plant, the amount of steam necessary to run the boiler has to be determined. To determine this a heat exchanger was modeled in Aspen plus with steam heating up solvent in the stripper. The steam used is Low pressure steam at 6 bar, giving a saturation temperature of 159°C. The steam stream enter the exchanger at 160 °C with a vapour fraction of 1, and exits the exchanger at 159 °C with a vapour fraction of 0. The amount of heat exchanged was then calculated on a per kg steam basis. to equate the reboiler duty to kg of steam. The price of steam was then set at 17 dollars/ ton as Ali et al. has used [22].

2.8.3 MEA Loss

An amine absorption plant will lose MEA continually through MEA volatility and potentially aerosol formation. Aspen plus gives the loss of MEA due to MEA vaporisation, however this does not account for the aerosols of MEA formed which escape trough the water wash. An estimation of the MEA loss was therefore made to be 10% of the MEA leaving the top of the absorber before the water wash. This would account for both MEA leaving the system and degradation.

2.8.4 Currency

This thesis uses USD 2022 currency. It is worth noting that the inflation for 2022 is higher than usual[28], possibly due to a global pandemic and war on European soil. This will make some prices much higher when converting from ie. 2017 currency to 2022 through inflation.

2.9 Fixed cost of production

Fixed cost of production are costs that are independent on how much the plant produces or how many operating hours the plant has.

2.9.1 Labour cost

the wages of the workers and supervisors are a part of the fixed cost of production. S&T suggest there is usually around 5 operators per shift position. Alkhayat and Gerrard have released a formula for estimating labour costs[29] shown in equation 2.18

$$N_{OL} = (6.29 + 31.7P^2 + 0.23N_{np})^{0.5} \tag{2.18}$$

Where

N_{OL} is the number of shift positions

P is the number of processing steps handling particulate solids, this is 0 for amine absorption

N_{np} is the number of non-particulate processing steps

N_{np} is given by equation 2.19.

$$N_{np} = \sum compressors + towers + reactors + heaters + exchangers \tag{2.19}$$

The number of equipment for the formula is listed in table 2.6. It is worth noting that this is not the list of major equipment, only the list of equipment used in formula 2.19 for calculating number of shift positions. N_{OL} for only the CO_2 capture is 2.7-2.8. Including the CO_2 compression this number rises to 3.3. The number of shifts is rounded to 3. three is also the number S&T suggest for a large site fluid processing plant.

Table 2.6: List of all equpment used in calculation of number of shift positions. *The number of towers vary between the 3-1 cases and the rest.

Equipment	**CO2 capture**	**CO2 Compression**
compressors		6
exchanger	3	6
heater	1	
towers	2-4*	
Total	6-8	12

For each shift position, approximately 5 operators are needed. This gives a four shift rotation, with time for weekends, vacations and holidays. Supervision is taken as 25% of operating labour. Direct salary overhead must also be included in labour cost, and includes cost of fringe benefits, payroll taxes, etc. The Direct salary overhead is usually 40% to 60% of the operating plus supervision. The formula for labour cost is shown in equation 2.20 The average pay for a system operator is $ 60,000 USD 2007 according to R&D and $ 67,000 USD 2017 according to Turton et al.s book Analysis synthesis and Design of chemical processes. These values equate roughly to 82,000 $ USD 2022 and is the worker pay used in this work. The formula for labour cost then becomes 2.21.

$$\text{Labour cost} = \text{operator pay} \cdot \text{shifts} \cdot \text{operator per shift} \cdot (1 + 0.25) \cdot (1 + 0.4) \tag{2.20}$$

$$\text{Labour cost} = \$\,82,000 \cdot 3 \cdot 5 \cdot (1 + 0.25) \cdot (1 + 0.4) \tag{2.21}$$

2.9.2 other fixed costs

The rest of the fixed costs are

- Maintenance, which includes the cost of the materials and labour, set at 4% of ISBL
- Property taxes, set at 2% of ISBL cost
- Rent of land and buildings, estimated at 2% of ISBL cost

- General plant overhead, Charges to cover human resources, finance, legal etc. This is taken as 65% over total labour costs

2.10 Sensitivity analysis

A sensitivity analysis is usually done for the key income and expense factors of a plant. This is to see how the economics of the plant will preform under different market trends.

As the cost of steam is the thing that will vary most from location, since the extra heat from industrial processes will vary a lot. NGPP can modify their plant to get cheaper steam for the reboiler, cement plants can salvage heat from the kiln. The base case for cost calculations use steam at full price. The sensitivity analysis modified steam costs down to 50 % of the price used. Norcem aims to only use excess heat from their cement kiln to have a capture rate of 50% in their upcoming large capture plant [30].

The steam cost is also upped to 120% cost. This is an indirect way of looking at increased electricity prices which could become a reality as discussed earlier.

The CO_2 tax negated in the base example is 59 dollars per ton of CO_2 which is the Norwegian tax on CO_2 [31]. Norway has stated that the CO_2 tax will steadily increase to 200 dollars at 2030 [32]. The CO_2 tax is then set to base at 59 dollar, 100 dollars, and the full 200 dollars per ton which it should have in 2030.

The simple payback time, and CO_2 tax necessary to break even on yearly expenses to the plant will be the two main ways to measure the different bla bla.

2.11 Pipeline and pumping cost

For transporting CO2, flue gas and amine, the pipeline material, diameter and thickness have to be known. The necessary material for the pipes are discussed in chapter bla bla. The pipes are only produced in a standardised set of diameters, and the closest one that fit the specifications have to be chosen. Pipes are sized in nominal pipe size(NPS), with the diameter and wall thickness given in nominal diameter (DN) and pipe schedule (SCH), and Each NPS has a corresponding DN. For pipes with NPS 14 (DN 350 mm), the DN will be equal to the outside diameter. For pipes smaller than NPS 14, the DN is not the always the outside or inside diameter, and the inside and outside diameters can be calculated after the wall thickness is known. This is shown in figure 2.4 The SCH is based on how much pressure the pipe must withstand, and is calculated by formula 2.22. Since the SCH is based on how much pressure the pipe must be able to withstand, and different pipe materials have different tensile strengths, each material will have different wall thickness for their schedule. Ie. a pipe with 14 NPS with SCH 40 will have a thicker wall if the material is cast iron, than a stainless steel pipe.

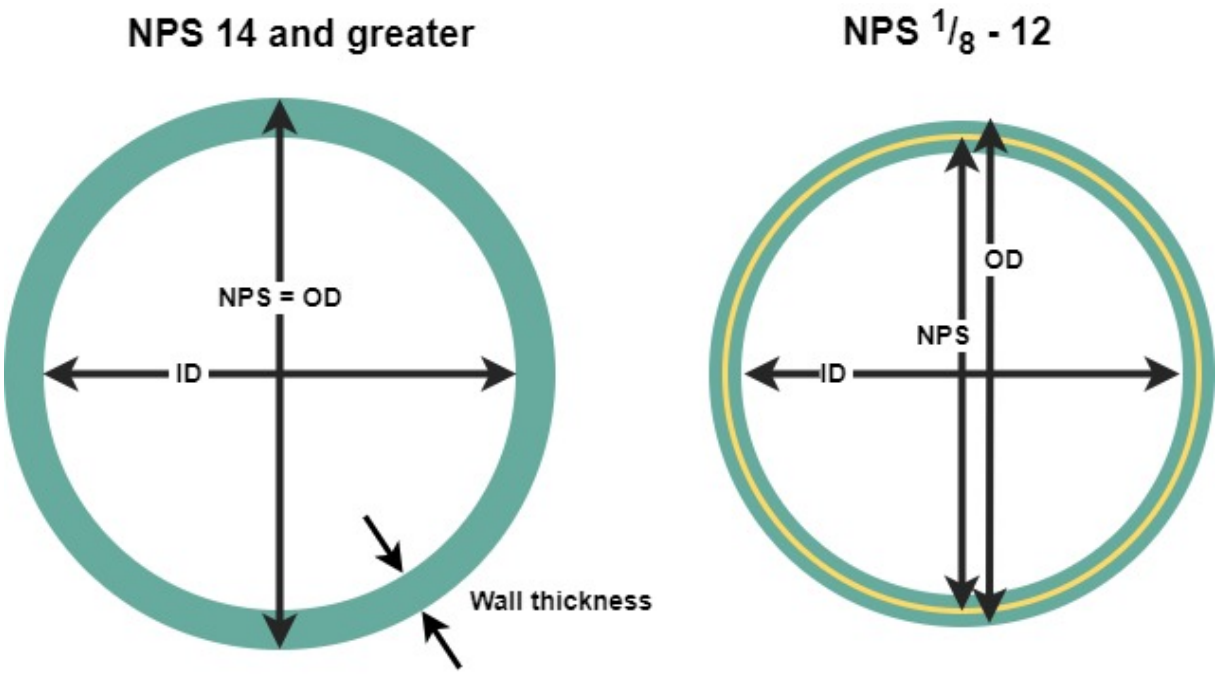

Figure 2.4: Pipe internal diameter, outside diameter, wall thickness and nominal pipe size for the different sizes of pipes.

$$\text{Schedule number} = P/S \tag{2.22}$$

Where:

P is the service pressure in (psi)

S is the allowable stress in (psi)

Aspen plus was used to calculate the diameter of the pipe with respects to finding the lowest size with acceptable pressure drop. To find an initial diameter for the pipe, a velocity based equation was used, eq 2.23. The velocity was set to 1 m/s for pumping liquids, and 15 m/s for gas in accordance to typical pipe velocities from S&T [33].

$$Diameter = \sqrt{\frac{4m}{v\pi\rho}} \tag{2.23}$$

Where:

m mass flow [kg/s]

v Velocity [m/s]

ρ Density [kg/m3]

The diameter was optimised from the inital diameter found in 2.23 to have a low enough pressure drop to be pumped several kilometers without having to be re-pressurised. Aspen plus economic analyser was then used to give an installed cost for the pipes. A list of the assumptions and specification for the pipelines are listed in table 2.7.

Table 2.7: Pipe specification

	MEA	**Flue**	**CO2**
Operating temperature [°C]	40	40	-25
Pipe schedule	10	10	40
Pipe material	304 SS	Cast iron	X 70 S
Pipe type	Welded		Seamless
pipe insulation	3 mm plastic coating		
Installation option	Buried 2 meter depth		

3 Model validation

To quantify and the uncertainty and quality of the simulations, the Aspen Plus model was validated against vapor-liquid equilibrium data and selected pilot plant runs.

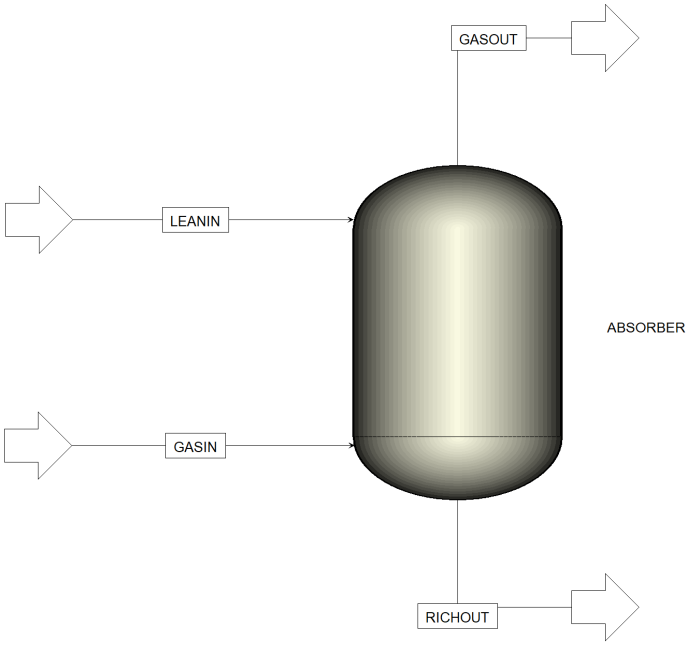

Figure 3.1: The case used in Aspen plus to validate the experimental vapour liquid equilibriums

3.1 Vapour Liquid Equilibrium validations

The simulated results are generated an flash column, with one inlet of 30 w% MEA called LEANIN, and one inlet of pure CO_2 named GASIN, shown in figure 3.1. The stream of CO_2 is varied to create different partial pressures of CO_2 inside the flash column, which gives different points to record the loading of the solvent. The validation is done for the temperatures 40-120 °C and for loadings in range 0.05-0.5. The temperature range is chosen because the absorber is usually run at 40 °C, and the stripper is operated at around 120°C, because of the thermal degradation of MEA [18]. The loadings range is from 0.05 to 0.5, as MEA has a maximum loading og 0.5 [17]. The simulated data is then compared to experimental data from Jou et al. [34], and is shown in figure 3.2. In table 3.1 the AAD for each temperature is presented

From figure 3.2, it can be observed that the deviations small.The AD is between 0.9 and 4.3 and the AAD is between 1.8 and 8.5 indicating a good fit between the Aspen Plus thermodynamic model and the literature data.

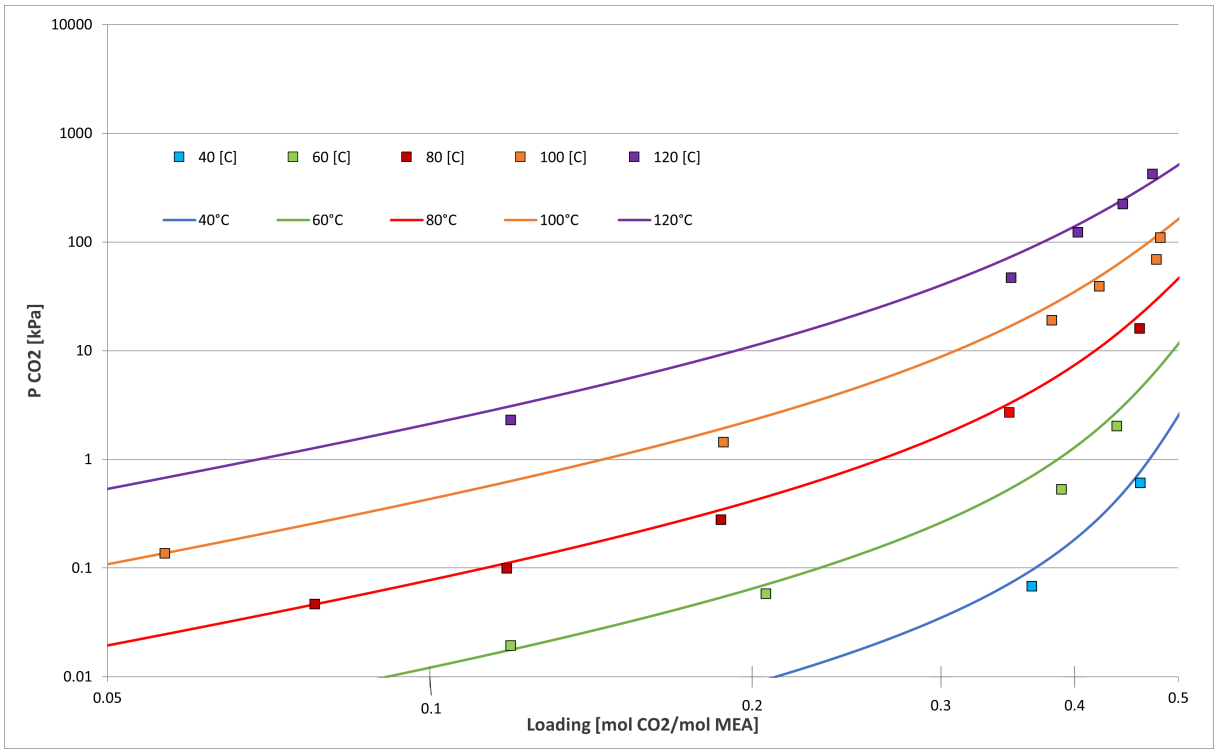

Figure 3.2: VLE data from Aspen compared with experimental results The points are experimental data from Jou et al. The lines are simulated values from Aspen plus.

Table 3.1: Average deviation and Average absolute deviation for the points in loading range 0.2-0.7 in the temperature interval 40-120 °C. $AD = \frac{1}{n}\sum_{i=1}^{n}|x_i|$, $AAD = \frac{1}{n}\sum_{i=1}^{n}|x_i - \bar{x}|$

Temperature	AD	AAD
40 °C	1,90 %	3,76 %
60 °C	4,32 %	8,15 %
80 °C	0,93 %	1,86 %
100 °C	4,26 %	8,52 %
120 °C	3,97 %	6,99 %

3.2 Pilot pland validation

This chapter presents pilot plant validations to quantify the uncertainty around the rate of absorption and desorption in packed columns.

3.2.1 Absorber validation

To validate the aspen plus model, data from two campaigns at NTNU and one at Sintef Tiller were used to validate the Absorber. The specifications for the plants and campaigns are listed in table 3.2. The absorber is modeled using a radfrac absorber, and the inlet conditions of the gas and liquid is set to the values reported in the articles for the campaigns. The amount of CO_2 captured and rich loading is then used to asses how accurate the aspen model is in its predictions.

Table 3.2: List of absorbers and specifications used for validation of the Aspen plus model. * This data is from an unpublished campaign

Author	**Tobiesen et al.[35]**	**Pinto et al.[36]**	Na*
plant	NTNU	NTNU	Tiller
packing Height [m]	4,36	4,23	15
Diameter [m]	0,15	0,15	0,2
Packing type	Sulzer mellapak 250Y	Sulzer BX	Sulzer Mellapak 2X
Loading range	0,18-0,41	0,25-0,35	0,16-0,47
experimental points	20	6	2

Figure 3.3 shows the difference in experimental and simulated values for rich loading for various lean loadings entering the absorber. The figure shows that most of the data points are above 1, meaning that the model will usually predict a higher CO_2 absorption rate than the real absorber. Most of the values of Sim/rich loadings are within a value of 1,05, which is a good accuracy for the results.

The difference simulated and experimental data for the amount of CO_2 captured is shown in figure 3.4. When comparing this figure and the figure for loading difference 3.3, data from Tobiesen and the tiller campaign have matching CO_2 loadings and CO_2 capture amounts, while the data from pinto shows very different predictions between loading and amount of CO_2 captured, this discrepancy is discussed below in 3.2.2 as it ties in with the temperature profiles found.

Table 3.3: Absolute deviation and Average absolute deviation for the rich loadings in the different campaigns

Author	Tobiesen et al.	Pinto et al.	Tiller
Rich loading AD	1,98 %	1,96 %	5,02 %
Rich loading AAD	1,81 %	0,32 %	0,69 %

3.2.2 Absorber temperature profiles

Temperature profiles inside the column from the simulations were compared with experimental values from Tobiesen and Pinto. The simulated temperatures from Aspen matched both the curves and exact temperatures for many of the experimental runs in the Tobiesen et al campaign, such as run 10 shown in figure 3.5. Half of the runs had similar accuracy of the simulated temperatures inside the column, where the error in prediction were below 1 °C. Run 5, 16 and 17 present themselves with notable deviations between simulated and experimental results, as seen in figure 3.6. In run 5, the profile does not match the results at all, and the difference in simulation and experimental data is higher than 4 °C for 2 of the points. This may be due to an error in temperature

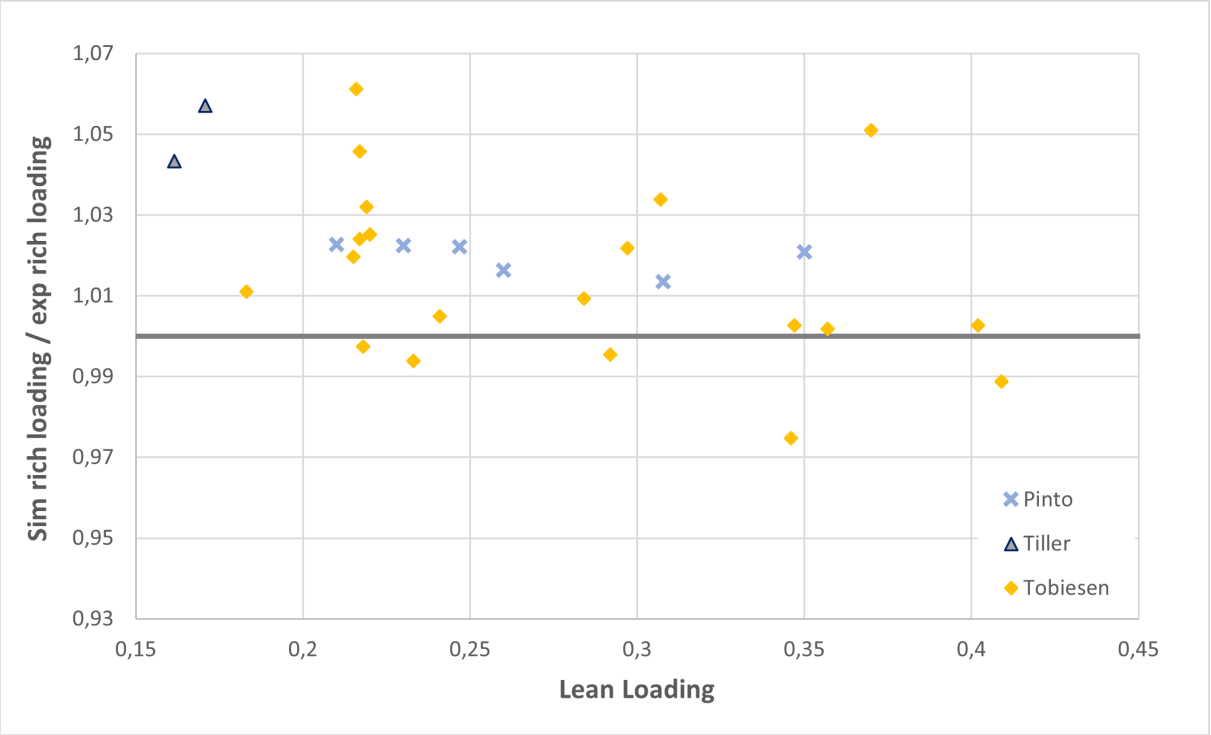

Figure 3.3: The difference in simulated value of the rich solvent plotted against the lean loadings in to the absorber

measurements in the experiment done by Tobiesen et al., as the experimental temperature profile inside the column is unlike all the other runs in the campaign. This run also has the largest deviation in term of rich loading from the absorber, and some other error in the experiment could be at fault. Simulation 16 and 17 have deviations in predicted and experimental values around 2 °C. The rest of the simulations had some deviation from the actual temperatures inside the column, but showed similar temperature curves inside the column, such as run 14 shown in figure 3.6, where the largest deviation in the column is 1,5 °C. These validations have also been done by Witzøe in a prevoius version of Aspen plus[37]. Her findings were in line with the ones described here.

For the Pinto et al. Campgaign, Aspen were not able to predict the temperature profile to any useful degree. The temperature profile of the column from run 1 is shown in figure 3.7, and all of the runs have equally inaccurate simulations results. Pinto's data also had a large discrepancy between loading and amount of CO_2 captured. Witzøe experienced similar inconsistency[37].

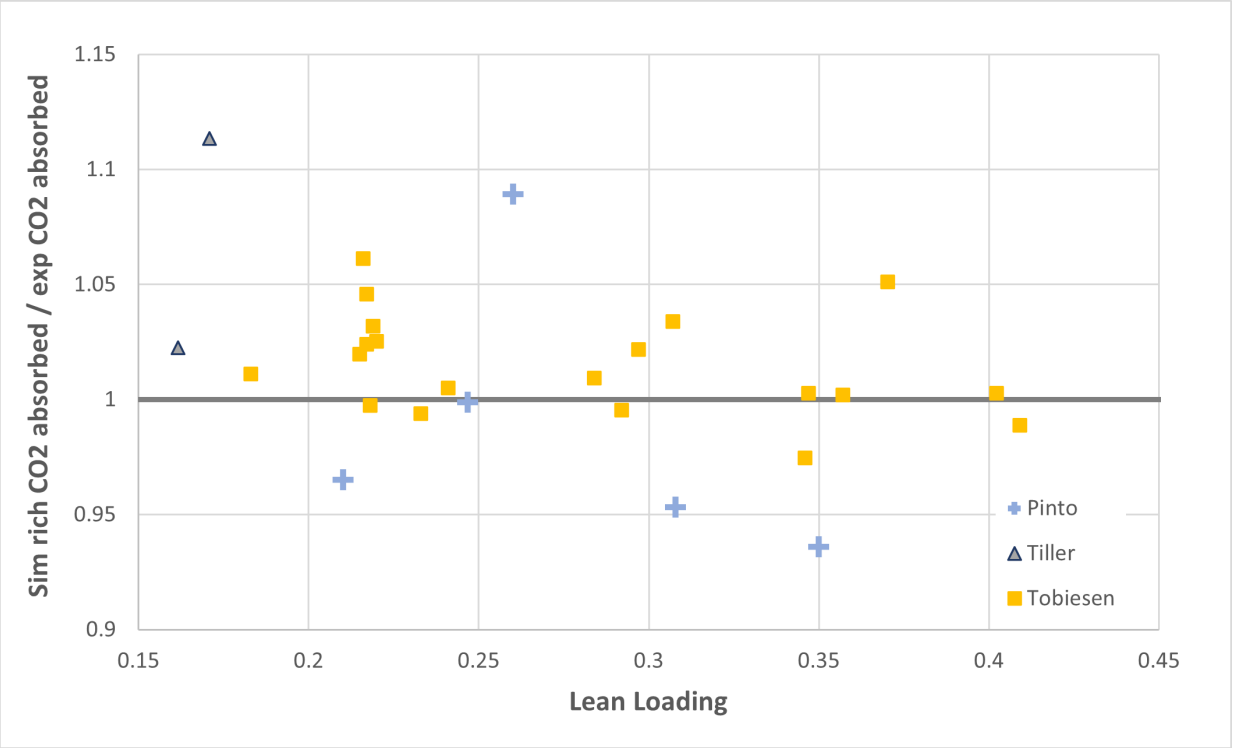

Figure 3.4: The difference in simulated and experimental value for amount of CO_2 absorbed plotted against lean loadings in to the absorber

3.2.3 Stripper validation

The stripper was validated against Tobiesen et al. desorber campaign[38]. The setup for the validation is depicted in figure 3.8, and the column specififcations are tabuletd in table 3.4 . The rich solvent RICHIN, stripper duty and condenser duty were matched with the experimental setup from the campaign, while the Lean loading in stream LEANOUT were compared against the experimental results.

Table 3.4: Stripper specification used for validation, Absolute deviation and Average absolute deviation between simulated and experimental lean loadings out of the stripper.

Author	Tobiesen et al.
plant	NTNU
packing Height [m]	3,89
Diameter [m]	0,1
Packing type	Sulzer mellapak 250Y
Loading range	0,46-0,22
Reboiler duty [kW]	3,9-11,6
experimental points	20
Lean loading AD	4,34 %
Lean loading AAD	4,17 %

The results of the stripper simulation is shown in figure 3.9. The results show that the

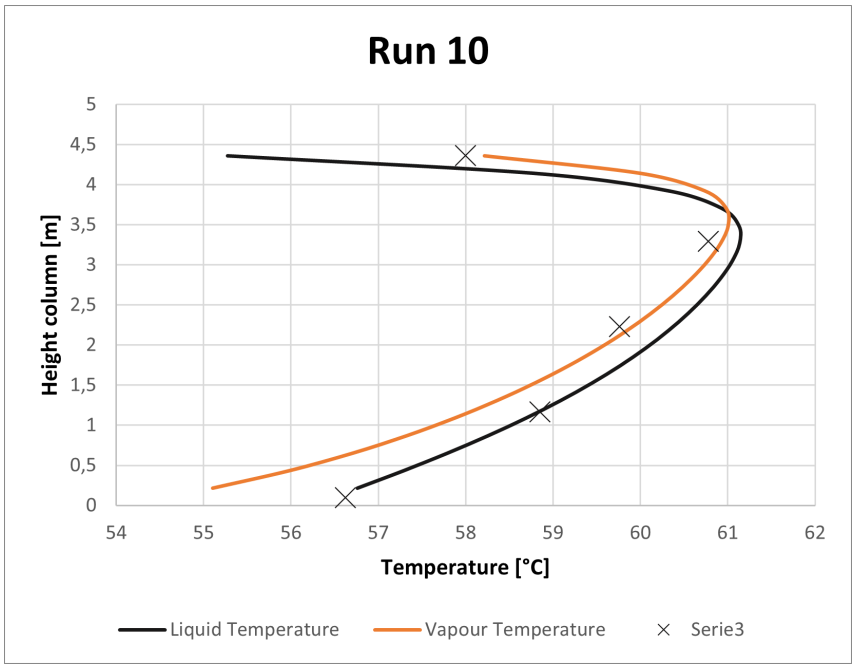

Figure 3.5: Temperature profile for the absorber in Tobiesen campaign run 10

model will give a higher desorption rate of CO_2 if the loading in is high, and lower rate of desorption if the loading is low. The break point seems to be around 0.35 loading. The Sim/exp lean loading is whthin 1.1 and 0.9 which shows good that the simulated values show good comparability with the experimental values.

All Aspen rate modeling options are included in appendix XX

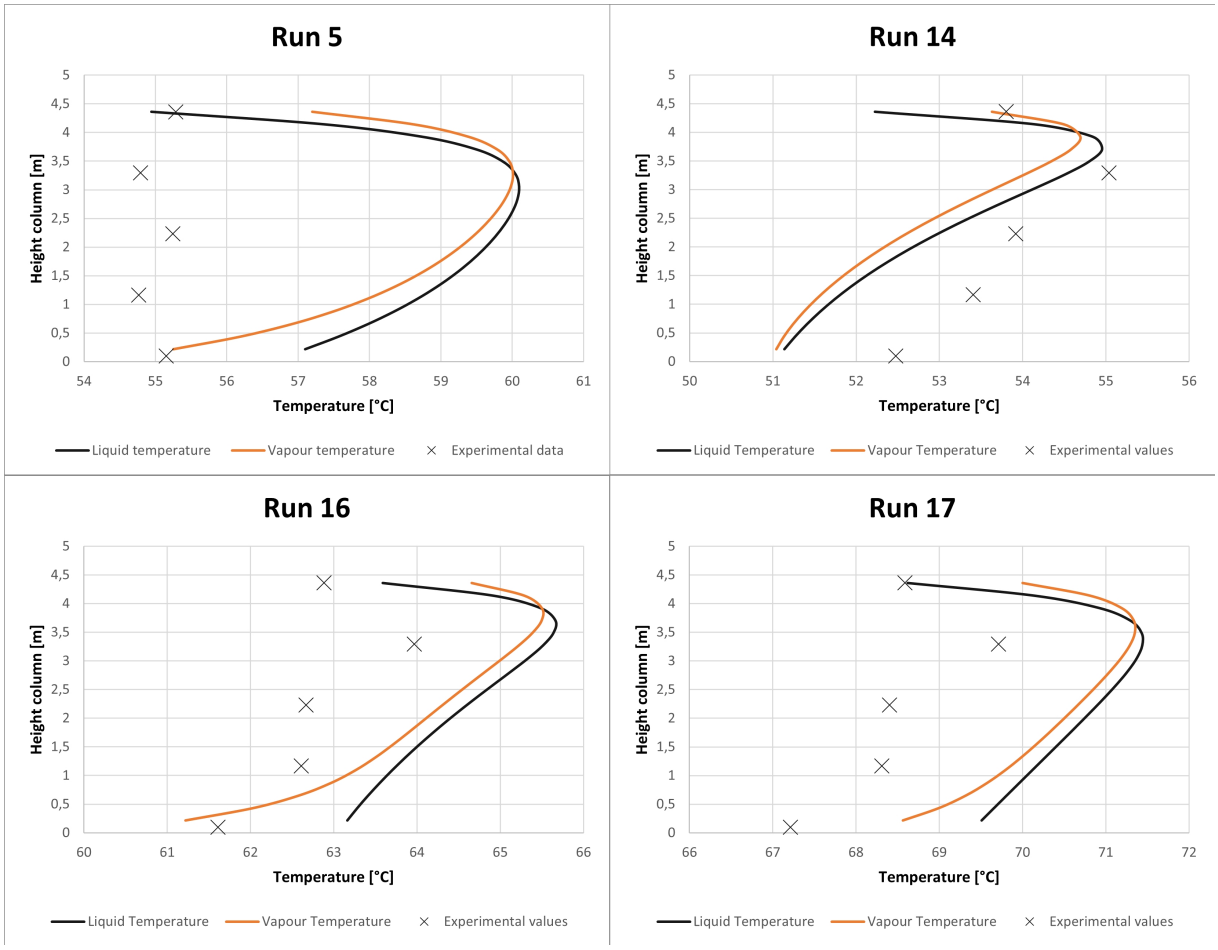

Figure 3.6: Temperature profile for the absorber in Tobiesen campaign run 5,14,16 and 17.

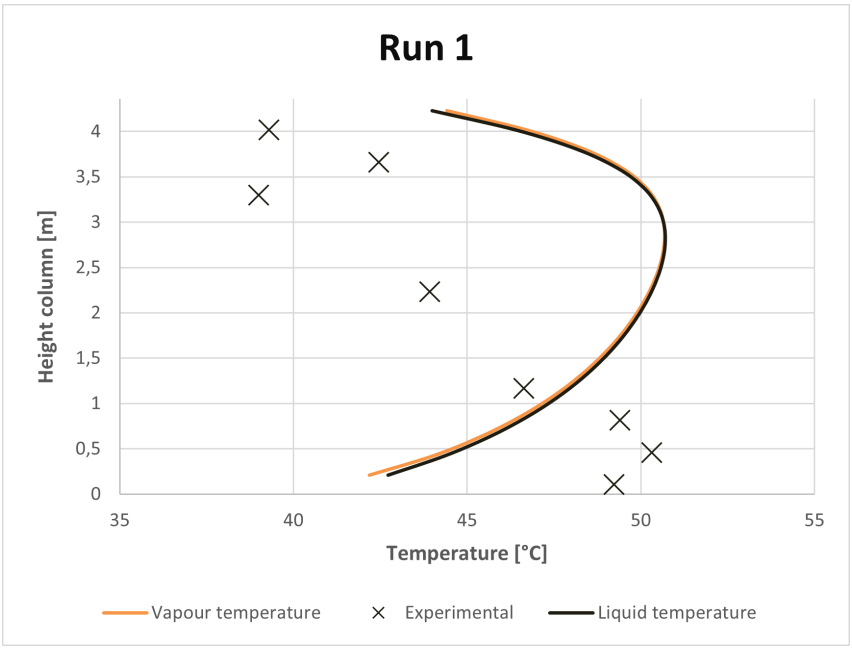

Figure 3.7: Temperature profile for the absorber in Pinto campaign run 1

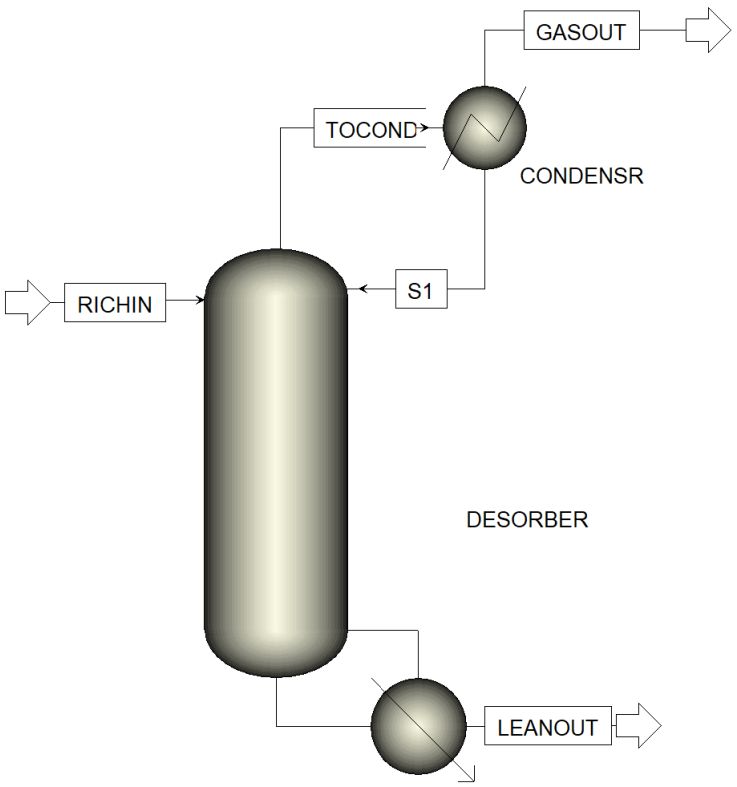

Figure 3.8: Setup for Stripper validation

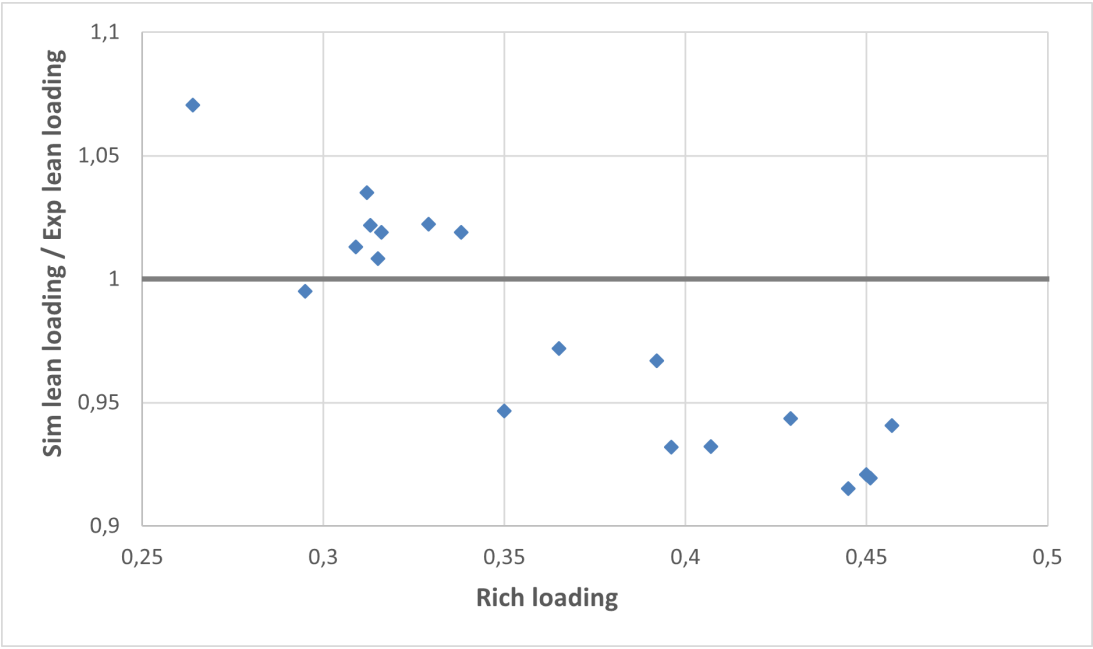

Figure 3.9: The difference in simulated value of the Lean solvent plotted against the rich loadings in to the stripper

4 Method

4.1 Industrial plants examined

CO_2 capture can be installed on many CO_2 emitters, such as natural gas power plants (NGPP) and cement plants. The industrial plants chosen in this thesis produce a range of flue gas amounts, with very differing CO_2 concentrations. With biogas having a small total amount of product gas and a large concentration of CO_2. Natural gas power plants have a large volume of flue gas, but with a low concentration of CO_2. Cement plants are in between biogas and NGCC power plants in terms of volume and CO_2 concentration of the flue gas. The NGPP and cement plant will have a capture rate of 90% while the biogas has a capture rate of 97% CO_2. the 97% capture rate is to meet the requirements for upgraded biogas[39].

Further the plants were categorized into small-medium- and large scales. The basis for deciding the size for the NGPP was the statistical average size of power plants in USA[40]. The plant size for the biogas are all large compared to the european average, but are comparable to some of the larger sizes found in USA[39]. In this study, relatively large biogas plants are investigated to better understand the impact of different CO2 concentrations in the gas phase on the costs of capture in industrial clusters. For small biogas plants, that impact on the overall costs would be too small. The cement plant is based on average size of cement plants in the USA[41]. The average was close to the Norcems cement plant in Brevik, and this was chosen as the medium sized facility. This would make it easier to validate the findings of the cost calculations later. The plant sizes are shown in table4.1.

Table 4.1: The Industrial facilieties with the gas ammount and concentration

	Plant		
	Biogas	**Cement**	**Natural gas**
	Methane [Nm3/h]	Cement annual [M tonne]	Poweroutput [MW]
Small	2500	0.8	200
medium	5000	1.2	400
Large	10000	1.6	800
		Gas CO2 dry%	
	40%	18%	4%
		Gas amount [Nm3/h]	
Small	4.2E+03	2.0E+05	5.0E+05
medium	8.3E+03	3.0E+05	1.0E+06
Large	1.7E+04	4.0E+05	2.0E+06

4.2 configurations

This thesis examine two different clusters which are composed of one biogas, one cement and one natural gas power plant, or one cement plant and one NGPP, these clusters are illustrated in figure 4.1. This thesis presents two different configurations for CO_2 capture on each cluster. The first is the standard case, in which each plant is equipped with their own absorber and stripper shown in figure 4.2.

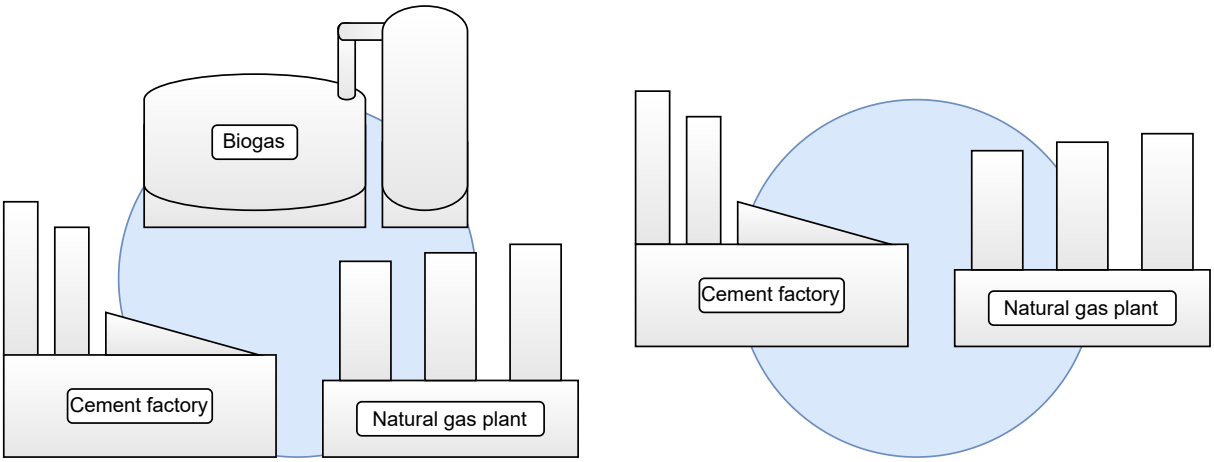

Figure 4.1: The two industrial cluster composition examined in this paper

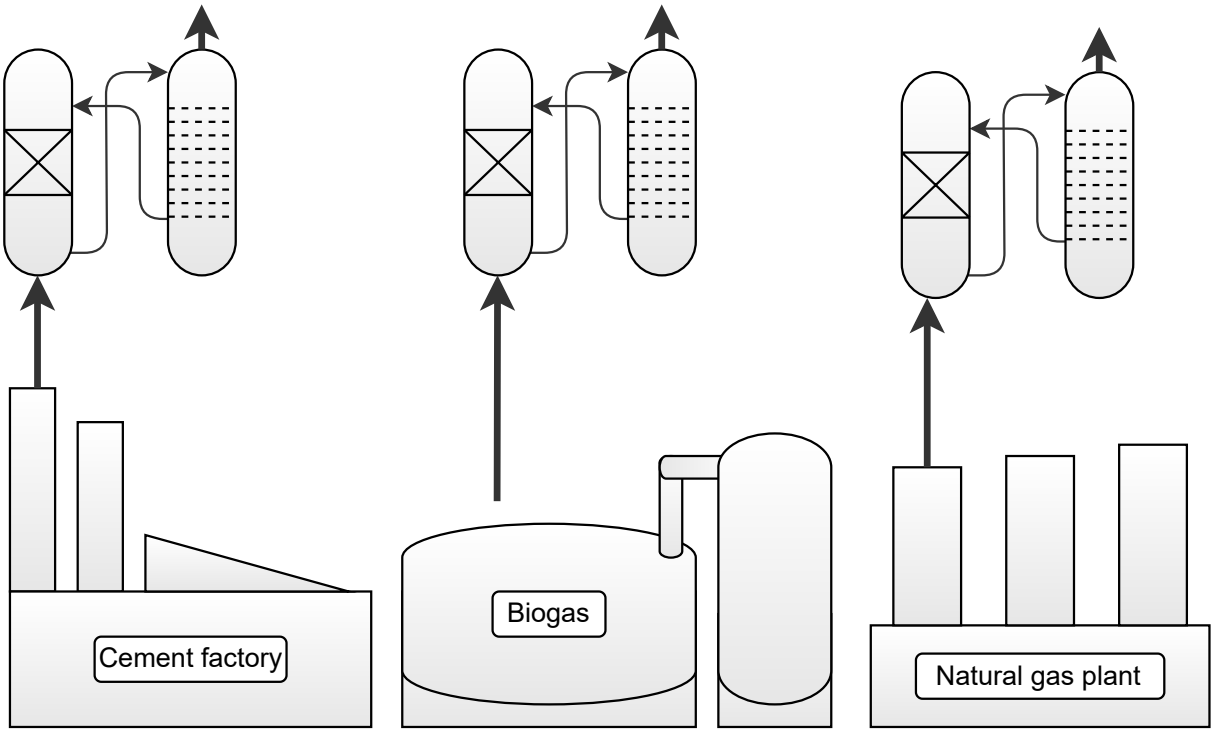

Figure 4.2: The base case for CO_2 capture, each plant has their own absorber and stripper

4.2.1 3-1 cluster

The second capture configuration is called 3-1 cluster and is a more novel configuration. Each plant is equipped with its own absorber, but all plants share a stripper as shown in figure 4.3. The rich solvent from each absorber must then be pumped to the central stripper. The stripper will boil off the CO_2 from all the absorbers, and the lean solvent can then be pumped back to the absorbers. The pros of this configuration is that no compression of CO_2 is needed on two of the plants, which is a large cost of CO_2 capture and storage[42].

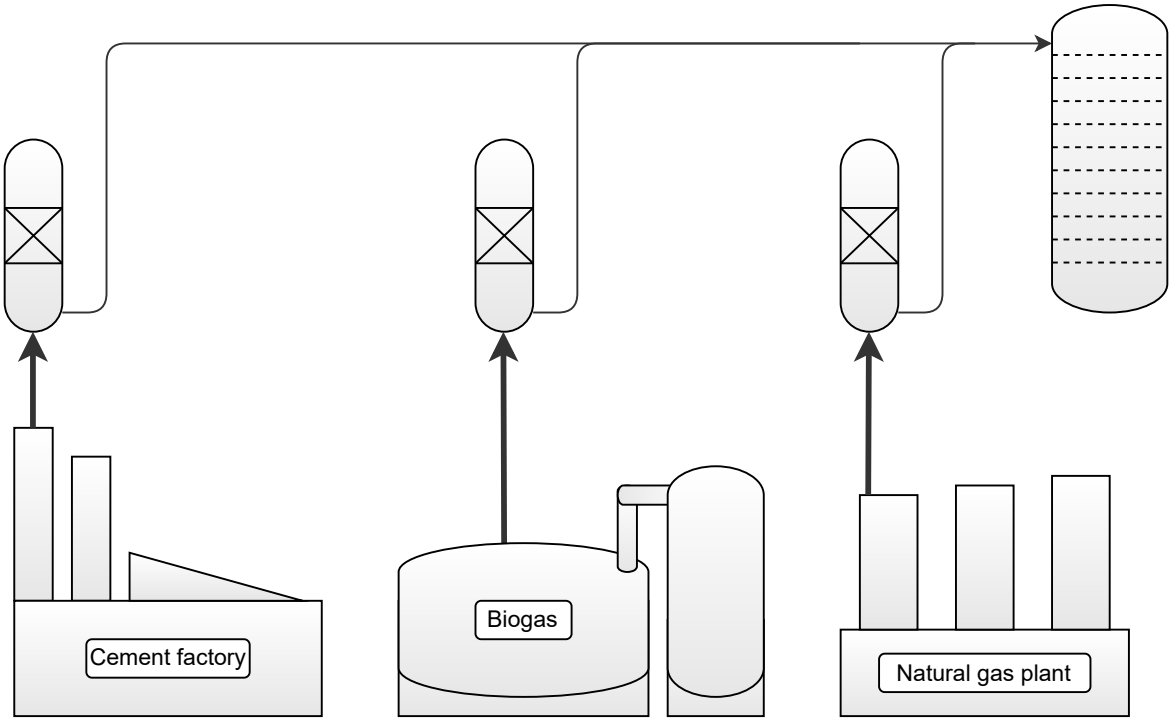

Figure 4.3: 3-1 cluster approach for capturing CO_2 3 absorber pump their solvent to one large stripper

4.2.2 1-1 cluster

The third capture approach would look at pumping the flue or product gas from each plant to one large absorber and stripper as depited in figure 4.4. This has the benefit of omitting both the absorber and stripper in one plant in favor of one larger absorber and stripper large enough to treat flue gas from both plant which is cheaper. The downsides of this design is the large pipes needed for the flue gas, and inefficient transport of gas with as little as 4 % CO_2 in the NGPP case. The reason the biogas plant is not included in this example is because the biogas needs its own absorber, as the methane in the product gas needs to be recovered and not mixed with flue gas.

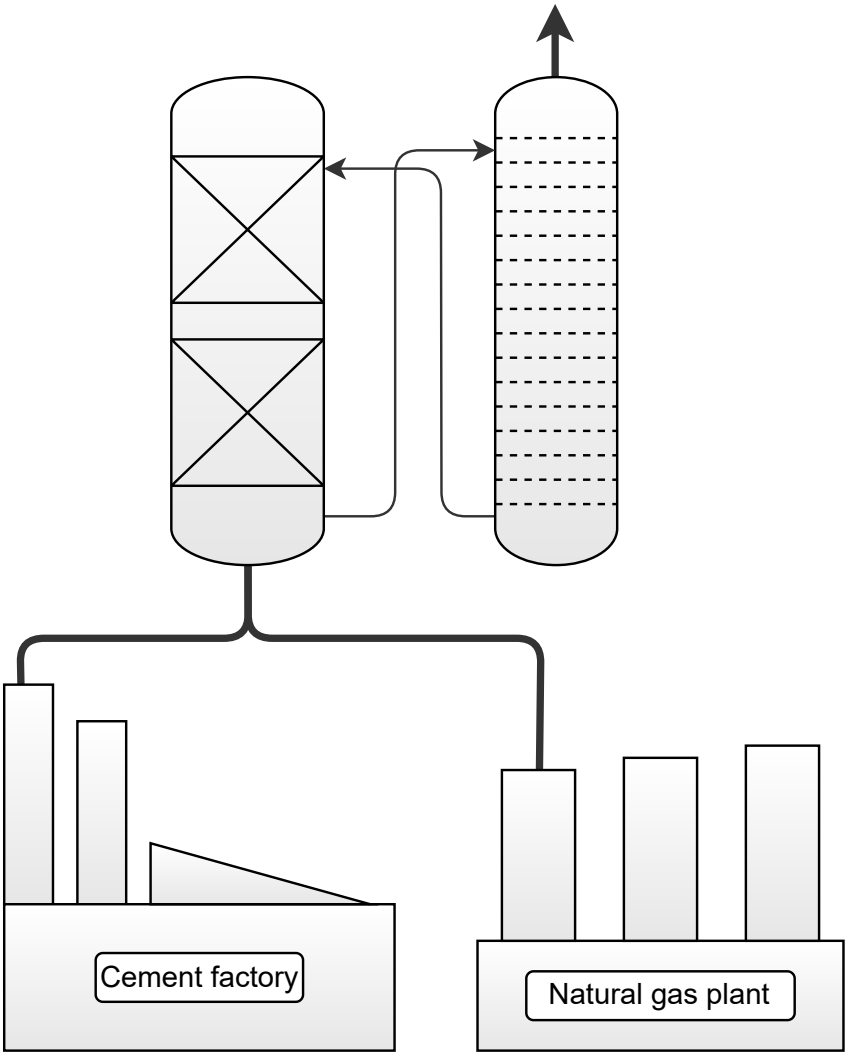

Figure 4.4: 1-1 cluster approach where the flue gas is pumped to one large absorber and stripper

4.3 Flowsheet

A simple flowsheet of the amine CO_2 capture process is illustrated in figure 4.5. The gas enter the bottom of the absorber and makes contact with the liquid solvent inside. The CO_2 in the gas reacts with the solvent and the solvent absorbs the CO_2 as the gas travels up the absorber. Once the gas reaches the top of the absorber the CO_2 has been removed from the gas and is now absorbed in the solvent. The CO_2 rich solvent exits the bottom of the absorber and is pumped to be heated in the heat exchanger and then to the top of the stripper. In the stripper the solvent is heated up to release its CO_2 content. The stripper is equipped with a reboiler that haeats the entire column, and a condenser at the top to condense out the water from the gas leaving the top of the stripper. The gas exiting the condenser is near pure CO_2 with trace amounts of nitrogen and water.

When the solvent exits the bottom of the stripper it is in its lean state. It is sent trough the heat exchanger to heat up the stream entering the stripper. The lean solvent is then mixed with water from the water wash, cooled and is ready to be sent in the top of the absorber to absorb more CO_2. the gas that exits the top of the absorber enters the water wash to remove volatile amines in the gas phase. In the water wash the gas is showered with water that absorbs volatile amines, with some of the water entering the absorber to ensure correct amount of water in the solvent.

To model this in Aspen plus several modifications has been done to the flow sheet to get results, these are detailed in appendix A.1 - A.4

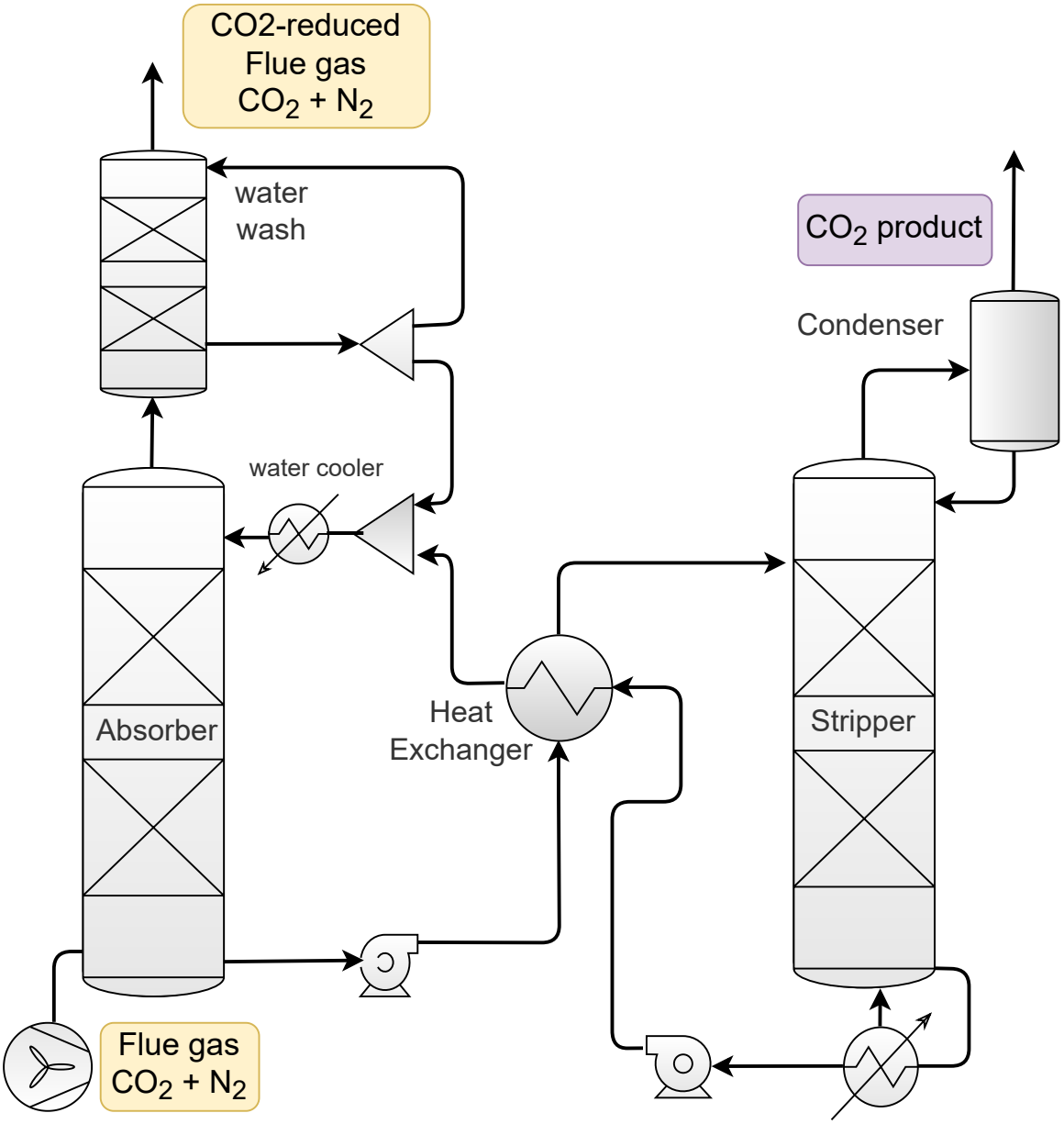

Figure 4.5: Flowsheet used for Amine absorption

4.4 CO_2 compression

The CO_2 has to be compressed before it is ready to be transported from the facility. Different levels of compression is needed based on the transportation method. For pipeline transportation CO_2 is liquefied to drastically lower the pressure drop in the pipeline[43]. To compress the gas to 150 bar several compressors are needed. This is due to the temperature increase of the gas as it is compressed. Due to mechanical constraints the max temperature of the compressor outlet is 120 °C and several compressors are needed[44]. This thesis uses 6 compressors to reach 150 bar, with a compression ratio of 2 for all steps except the first. The different pressures after each compression is shown in figure 4.6 which depicts the compression train. In the simulations the last compression is up to 150 bar which is an oversight. The CO_2 only needs to be compressed to 110 bar to reach its supercritical state. Once the CO_2 is in its supercritical state it can be further pressurised in a pump. This will likley not impact the results too much, as 6 compressors would still be needed to compress the CO_2 to its liquid state. Other papers have found different compressor amounts, Ali used 4 compressors reach 96 bar[22], while Biliyok found used 6 to reach 110[44]. Biliyk state they use thermal limitations of 120°C and a maximum poly-tropic head of 3050m per compression stage / impeller[44]. Ali use a maximum outlet pressure from the compressor at 160 °C.

For compressing the CO_2 to lower pressures than needed for the supercritical state, the price of the plant can be halved or divided by a factor to find the cost for a lower compression. this can be done as the individual compressor prices are very similar to each other. Ie. later in this thesis an example of CO_2 compressed to 20 bar is used, that means three compressors would be needed. The price for this would be 50 % of the full cost compression.

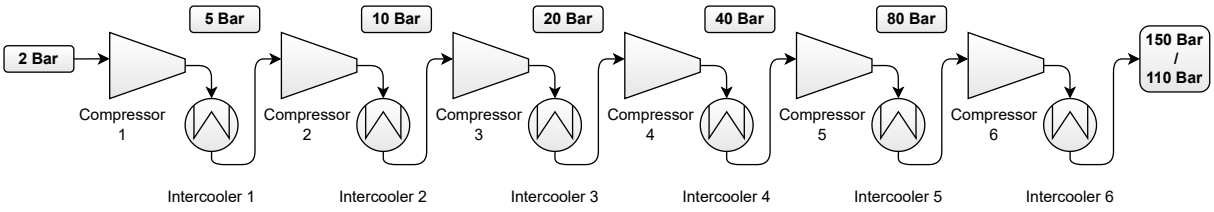

Figure 4.6: Compressor train compressing the CO_2 to 150 bar for transport or storage

biogas intercooler

4.5 design specifications

As a process can be optimised to the near infinite, several design factors for the system has been predetermined ahead of modeling to efficiently arrive at meaningful results about the different system configurations (((rewrite I think))).

4.5.1 Absorber

The diameter in the column is calculated by equation 4.1 based on the gas velocity through the column. The diameter is adjusted to make the gas velocity 2 m/s. 2 m/s is suggested as an optimal gas flow in terms of cast for aCO_2 absorption column using 30weight% MEA by Park and Øi[45]. In the paper they use a gas with 3.73% CO_2, and for the simulations with similar concentrations of CO_2 (3.7 - 7.5)% this yielded good results. For concentrations at and above 16% however, Aspen plus reported flooding in the ranges 90-120%. Aspen plus use their own Aspen-Wallis correlation to calculate flodding and pressure drop through the column, for which they have not published the correlation parameters[46]. It is likely that the correlation uses liquid amount, as that is the main thing that varies with the cases from low to high concentration CO_2. The low concentration CO_2 use 0.8 kg of solvent per kg gas, while the higher concetrations use 3.3 kg up to 7.1. The absorbers with CO_2 concentrations from 3.7 to 7.5% had a diameter based on gas velocity equal to 2 m/s, while the absorbers with higher concentrations had the diameter calculated based on reaching 80% flooding. The absorber diameters and gas speed through column are shown in table 4.2

$$D = \sqrt{\frac{4\overline{V}}{\pi \cdot v}} \tag{4.1}$$

Where:

$\overline{V}$ Volume flow of gas through colum $[m^3/s]$

v gas speed through column, equal to 2 $[m/s]$

Table 4.2: Absorber diameters and gas spees through columns

	Plant							
Size	**Biogas**		**Cement**		**NGPP**		**1-1 Cluster**	
	D [m]	v [m/s]	D [m]	v [m/s]	D [m]	v [m/s]	D [m]	v [m/s]
S	1	1.7	7	1.7	9.8	2	11.9	2
M	1.5	1.7	8.3	1.8	13.9	2	16.3	2
L	2	1.7	9.5	1.8	19.7	2	22.1	2

Biogas intercooler

As the absorption of CO_2 is an exothermic reaction, the absorption of CO_2 increases the heat of the absorber. This increase in heat becomes an issue for the biogas absorption, as the temperature increase reached ** °C in the simulation. Therefore the biogas was

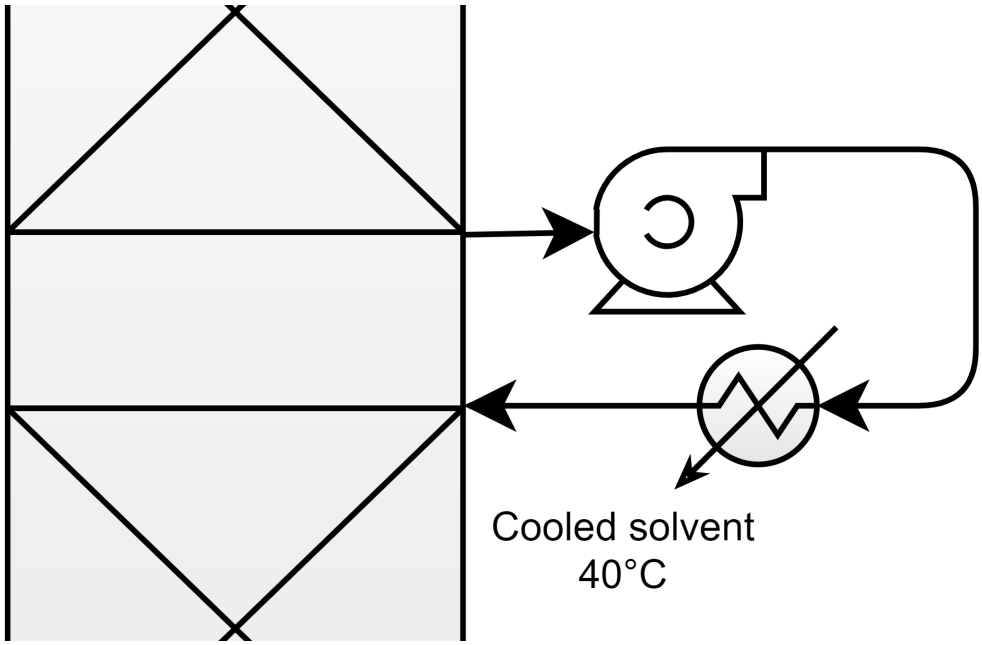

Figure 4.7: Biogas intercooler

fitted with an intercooler, which cools all the solvent in the middle of the absorber to 40°C as depicted in figure 4.7.

4.5.2 Loading and solvent amount

As the reboiler duty is by far the highest running cost in the plant, making sure this is at a minimum is important. To find the lowest reboiler duty possible, the capture rate was set at 90 % (or 97% for biogas) while solvent amount was varied. As the differen plant types have varying levels of CO_2 the amount of solvent necessary will vary. Results for the medium NGPP is shown in figure4.8 with specific reboiler duty (SRD) and loading plotted against L/G. The low point for SRD in the plot can be observed at around L/G = 0.83. After this point the increasing solvent amount does not lower the reboiler duty, and the duty will start to increase as the solvent amount is increased. The absorber will then be run with a L/G equal to 0.83, as this is the most effective in terms of reboiler duty. As the gas speed through the column is constant throughout the different sizes, the optimal L/G can be expected to remain constant with the different sizes of the plant. This is confirmed in figure 4.9. The slight variations are most likely due to slight discrepancies in solvent concentration capture rate.

The SRD plot for the different facilities are shown in figure 4.10. The SRD low point for each facility is tabulated in table 4.3

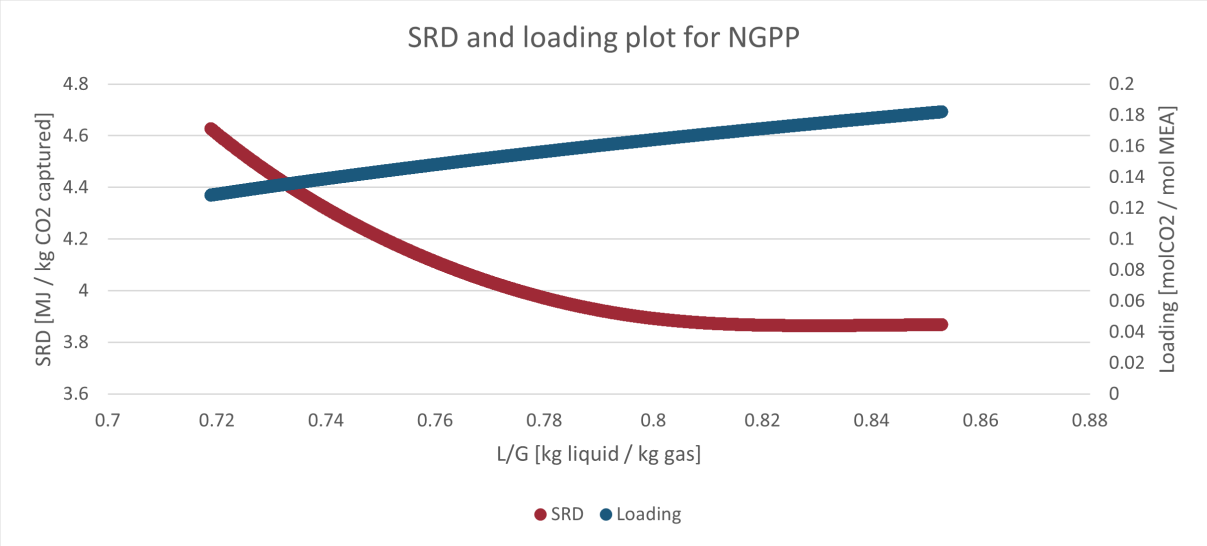

Figure 4.8: SRD and loading plot for medium sized NGPP

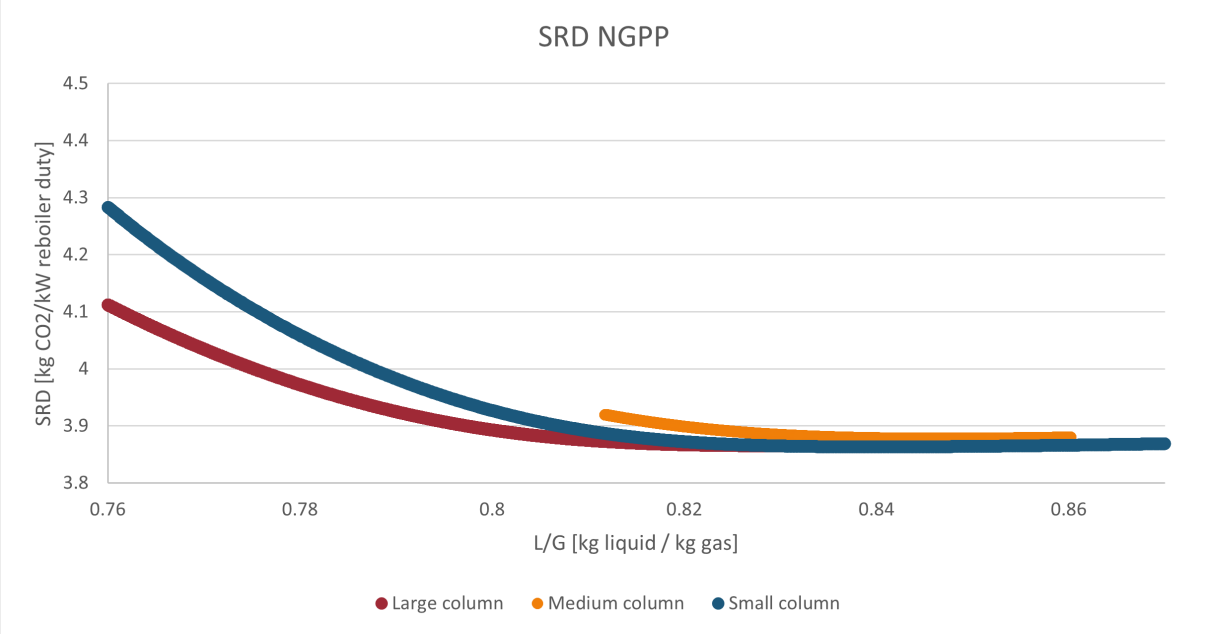

Figure 4.9: SRD plot for the small, medium and large NGPP column, done to validate that the column scales correctly

Table 4.3: SRD low points for each facility

Facility	SRD [MJ / kg CO2 captured]	Loading
Biogas	3.6	0.12
Cement	3.7	0.17
1-1 Cluster	3.8	0.17
NGPP	3.9	0.18

Table 4.4: Specifications for the flow sheet * The Solvent concentration and capture would vary within 1 % in the different simulations, this is detailed in appendix

Specification	Value
Watercooler water inlet	15 °C
Watercooler water outlet	40-50 °C
Pump efficency	0.7
Compressor efficniency	0.7
MEA concentration	30 weight% ± 1% *
Solvent inlet temp	40 °C
Flue gas capture %	90 % ± 1% *
Biogas capture %	97 % ± 1% *
Column packing	Mellapak 250 Y
Column heights	15 m
Flue gas inlet temp	40°C
Absorber pressure	1 bar
Stripper pressure	1.8 bar
Stripper diameter	Same as absorber
Reboiler temperature	∼ 120 °C

4.5.3 Heat exchanger

The heat exchanger heats up the rich solvent (COLD-IN) before the stripper and cools down the lean solvent (S13) for the absorber, depicted in figure 4.11. The exchanger was specified to have a 10 °C temperature difference between the hot inlet stream coming from the stripper (S13) and the cold outlet stream heading in to the stripper (COLD-UT). The rich solvent is higher pressure (8 bar) to avoid bubbling inside the heat exchanger as the solvent heats up and it loses its affinity to CO_2.

The remaining flow sheet specifications are tabulated in table 4.4.

4.6 pipeline

One important question regarding the clusters, is how close do the emission sources have to be for it to be economically advantageous to join them on the same capture facility? another question is how the facilities should be connected. What is the difference between pumping the flue gas from a plant and pumping CO_2 rich solvent from an absorber on the same plant? and how does these parameter change in varying flue gas amount and CO_2 concentration.

4.6.1 MEA transport

As MEA is corrosive, the steel pipes have to be high grade steel to avoid excessive corrosion and pitting of the pipe. Hjelmaas et al. have ran an MEA absorber with different "testing plates" inside to examine what steel can be used in the construction of MEA absorbers and Strippers[47]. This will be applicable to what grade steel the pipeline will have to be. The paper found that steel 304S stainless steel is necessary to avoid excessive pitting in the steel. The MEA pipeline also has to be two pipes, to pump the lean solvent from the stripper back to the absorber. The advantages of transporting MEA is that it is that the CO_2 is in liquid form, giving much lower costs of pressurising the stream, due to pumps being much cheaper to buy and operate opposed to compressors.

4.6.2 CO2 Transport

For CO_2 transport over longer ranges the gas is liquefied to drastically lower the pressurisation costs.it is suggested that for pressurised co2 transport a pressure from 80 - 110 is needed to keep the co2 liquefied during transport[4]. This leads to a higher grade of steel needed for the strength necessary to withstand the higher pressure. GAO et al. uses a X 70 S steel pipe with SCH 30 to transport CO_2 at 150 bar[43].

For flue gas transportation Cast iron can be used due to the flue gas not being corrosive or high pressure. This leads to the flue gas pipeline to be much cheaper in terms of material costs. However, due to the lower CO_2 concentration of the gas, the volume of gas is much higher, thus much larger pipe diameter is needed to transport the same amount of CO_2. The gas also needs to be compressed to be transported through pipes, which is expensive both in purchase of the compressor, as well as in electricity usage compared to pumping liquids.

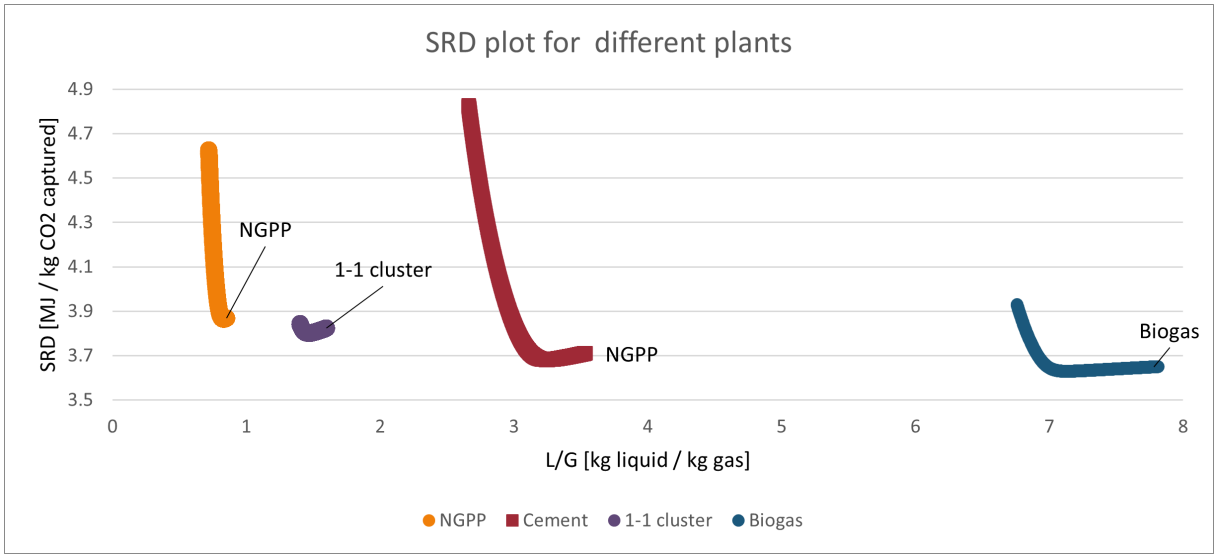

Figure 4.10: Caption

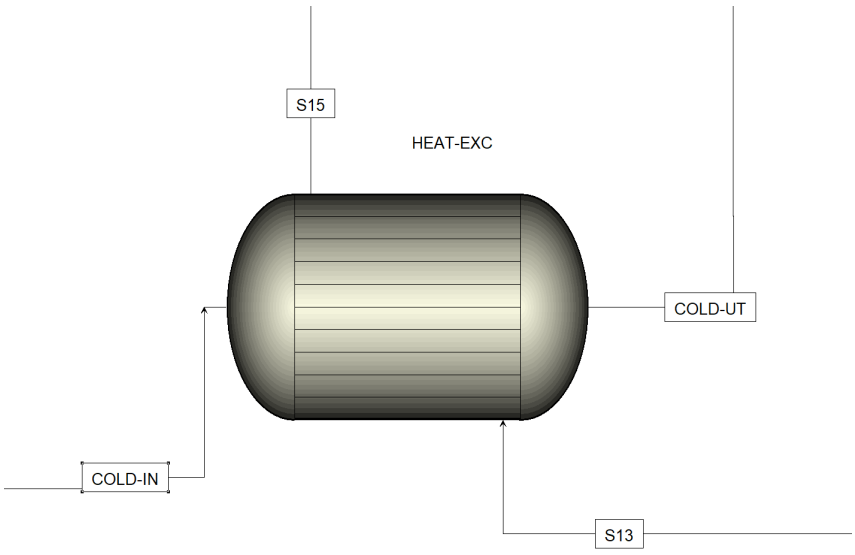

Figure 4.11: Lean/rich solvent heat exchanger

5 Results

5.1 medium sized cement capture plant

This chapter will provide an in depth overview of the results for the medium sized cement plant. This cement plant has the same size and production capacity as Norcems cement plant in Brevik. As there is much research and public records of this plant it is the best plant to go into detail to. Only a summary of the 14 other plant configurations will be presented in the main results.

5.1.1 Capital cost

The cost of all the major eqipment is estimated using Sinnot and Towler's cost correlations described in chapter 2.6. The material costs and sizing parameter for the medium cement plant is shown in table 5.1. The purchased equipment cost is used to estimate the ISBL cost for the facility using the Hand factor, Lang factor and Sinnot & Towler factor. The ISBL and total capital cost for the plant are tabulated in table 5.3.

Table 5.1: Size parameter and material cost for each major equipment in the medium cement CO_2 capture plant in 2007 USD.

Equpiment	**size parameter**	**size**	**Cost [$ MM]**
Absorber	Wall mass [kg]	126169	1.49
Stripper	Wall mass [Kg]	230313	2.47
Water wash	Wall mass [Kg]	25234	0.39
Column packings	cubic meters [m3]	1786	2.96
Lean & Rich solvent heat exchanger	Area [m2]	18550	3.84
stripper condenser	Area [m2]	1285	0.27
lean solvent cooler	Area [m2]	739	0.15
Reboiler	Area [m2]	2887	1.64
Pump from absorber	Flow [L/s]	341	0.18
Pump from stripper	Flow [L/s]	341	0.18
Cooling water pump	Flow [L/s]	676	0.32
Flue gas fan	flow [M3/h]	313679	3.07
Total			19.24

As figure 5.1 shows, the most expensive equipment by far is the heat exchanger. The percentage cost of each unit was compared to other works: Nwaoha et al. Have investigated CO_2 capture for the same size plant as this one[26]. Ali et al. present CO_2 capture for a cement plant with equal size to the small cement plant from this thesis. The high price percentage of the heat exchanger is similar to the other works. Nwaoha and Ali present very different prices for their absorbers, which makes it hard to compare

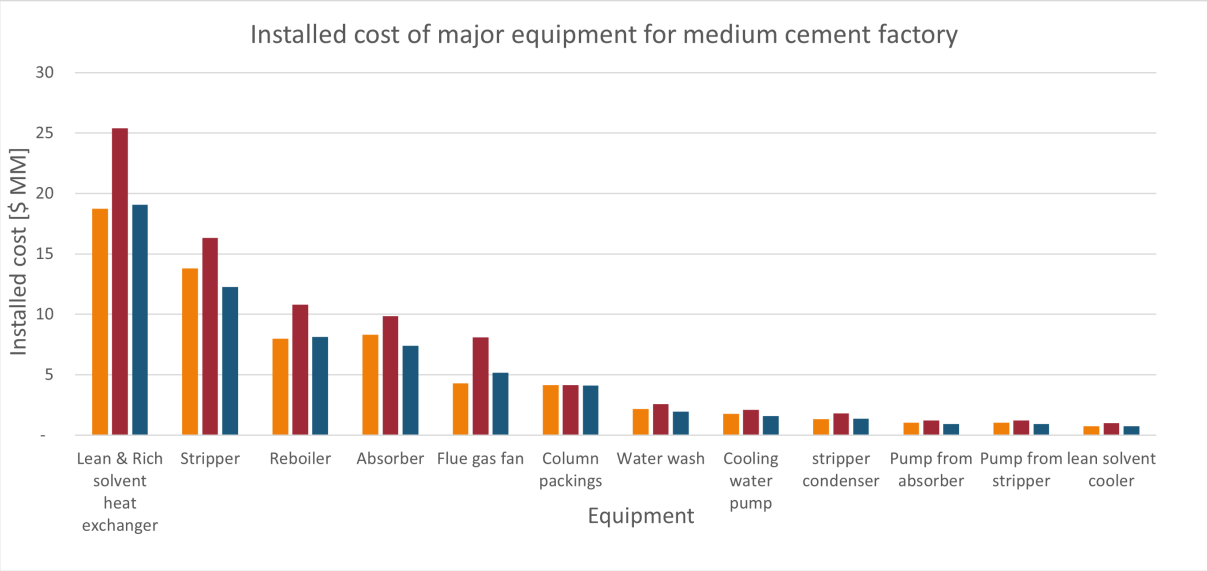

Figure 5.1: Installed cost of major equipment using Hand, Lang and Sinnot & Towler factors

the price of the absorber. One note able thing is that Ali's reboiler is nearly a third of the investment cost, and NWaoha does not state the individual price of the reboiler or stripper vessel, making it difficult to compare this. The stripper is probably oversized when looking at the relative diameter between the absorber and stripper. Both works have much smaller diameter in their stripper, than their absorber, while this work have the same diameter for both columns. This will impact the cast savings for the 3-1 scenario the most, as it effectively investigates the savings from removing two of the strippers from the system. The other works have their flue gas fan at 1-2 % of the equipment cost, while in this calculation it accounts for 7% of the cost. This means the fan is probably overpriced in this work.

Table 5.2: Cost percentage for major equipment for co2 capture from other works

Equipment	This work	Nwaoha	Ali
Heat excanger	34%	22%	47%
Absorber	25%	54%	14%
Stripper	30%	20%	3%
Reboiler	2%		32%
Pumps	2%	3%	3%
Transport fan	7%	1%	2%

The total capital cost is estimated between 184 and 314 $ MM. This is similar to the original cost estimation Norcem presented for their facility at 330 $ MM (3,3 B nok) [48]. The Norcem CO_2 capture plant will only capture roughly 50% of the CO_2 from their process. This due to their goal of supplying all the heat for stripping the solvent from surplus heat from their process [30]. The price estimate has later been increased estimate

Table 5.3: ISBL and total capital cost for the medium sized cement plant and for compression of the CO_2.

	ISBL [$ MM]		
Factor	**CO2 capture**	**CO2 compression**	**Capture and compression**
Hand	56	38	94
Lang	89	72	161
S & T	66	46	112
	Total capital cost [$ MM]		
Hand	109	75	184
Lang	173	141	314
S & T	129	90	218

to 430 $ MM due to several reasons, among them: increased market prices, increased labour cost and increased electricity cost[49]. It would make sens the cost estimation from Norcem is higher than the one presented her, as they include the cost of retrofitting the cement process to deliver heat to the reboiler. Even though the Norcem plant will only capture 50 CO_2, and they include the cost of retrofitting, the sizing and cost estimation done in this thesis provide a similar price for the plant.

5.1.2 Running cost

The Power used in for the major equipment are shown in table 5.5. The pumps and fans use electricity, while the reboiler duty is converted to kg steam.

Table 5.4: Running production cost and for the medium cement plant

Expense	Value	Price	Cost [USD/hr]
Steam	44 [kg/sec]	17 [$/ton]	2,692
Electricity, capture	1690 [kW]	0.08 [$/kWh]	135
Electricity, compression	8565 [kW]	0.08 [$/kWH]	685
Mea	0.04 [m3/hr]	1866 [$/m3]	70

The running cost of the plant can be divided into production cost which directly linked to the amount of CO_2 captured, and fixed costs which are independent of how much CO_2 is captured. The production costs are Electricity, steam and replacement of MEA. How these values are calculated are detailed in chapter 2.8. The results for this plant is in table 5.4.

Table 5.5: Running production cost and for the medium cement plant

Equipment	Power usage [kW]
Pump from stripper	8
Reboiler duty	92390
Pump from absorber	380
Flue gas fan	1292
pump for cooling water	8

The fixed cost of production are summarised in table 5.6. The maintence, property taxes and rent of land are related to the capital cost of the plant, a larger plant would mean higher expenses on these costs, while labour and overhead will stay the same.

Table 5.6: Fixed costs for the medium cement plant with and whitout co2 compression

Expense	Cost [$ MM / yearly]	
	without compression	with compression
maintenance	2.6	4.5
Total labour cost	1.5	1.5
property taxes & rent of land	4.0	5.8
General overhead	0.6	0.6
Sum	8.8	12.5

The total cash flow for the cement plant is shown in table 5.7. This shows that the plant will have a positive cash flow if the cost of compression is disregarded. If the CO_2 compression is added to the costs the plant will have a negative cash flow.

Table 5.7: Cash flows for medium cement plant with and without compression of CO_2

	Withouth comp. [$ MM / yearly]	**With comp. [$ MM / yearly]**
Expense	35.5	45.5
Income	41.8	41.8
Sum	6.3	-3.6

The cost of capturing CO_2 was found to be 64 \$/tCO_2 with CO_2 compression. Ali et al. have investigated a similar size plant with 85% capture and present the cost at 62 €/ tonne in 2019, giving 80 \$/tCO_2 in 2022 \$[22]. Nwaoha et al. present 92 \$/tCO_2 with 90% capture in 2018, giving 106 \$/tCO_2 in 2022 \$[26].

5.1.3 Pumping and pipeline cost

The installed costs for pipelines used for the medium cement plant is tabulated in table 5.8, and the pressurising cost presented in table 5.9. The size of the pipe is set to give a pressure drop of approximately 0.5 bar/ km for the MEA and flue, and 0.1 for the CO_2. The lower pressure drop for the CO_2 is because the liquefied CO_2 has a more expensive compressor, than the inexpensive pump used to pressurise the solvent.

The pipe sizes can be changed to better suit specific examples. This is demonstrated in table 5.10, where the pressure drop and cost of the pipeline are given for 3 different pipe sizes. Depending on how far the MEA will be pumped, and if there are plans to use the same pipe to transport solvent from multiple plants, and must be tailored to each case.

Table 5.1 5.9 shows that although the MEA has the most expensive pipeline, the cost in electricity for pumping is a fraction of the cost to compressing the gas for transport. The MEA pipes and CO_2 pipes have very similar pumping costs, although the MEA pipes have a substantially higher cost for the pipelines. This is due to the larger size of pipeline, and the fact that MEA needs two pipes pumping the solvent both directions.

Table 5.8: Installed cost of pipelines

Type	**[$ K/km]**	**NPS**	**Delta P [bar/km]**
flue	1,675	36	0.60
MEA	2,918	20	0.49
CO_2	825	10	0.07

Table 5.9: Cost of pumping the gas

Pipeline type	Electricity /km	Compressor or pump cost [$ K]
CO2	0.1 [kW/km]	1,372
FLUE	1420 [kW/km]	7,027
MEA	2.6 [kW/km]	46

Table 5.10: Variations in price and pressure drop

Type	[$ K/km]	NPS	Delta P [bar/km]
MEA	2,019	18	0.82
MEA	2,426	20	0.49
MEA	3,195	22	0.30

5.2 Results summary

Table 5.11: The average total capital cost for the different facilities without and with CO2 compression

Without compression [$ MM]			
Facility	**Small**	**Medium**	**Large**
Biogas	5.2	8.6	14.3
Cement plant	97	137	188
NGPP	142	260	493
3 - 1 Cluster	395	349	646
1 - 1 Cluster	225	383	675
With compression [$ MM]			
Biogas	43	52	65
Cement plant	183	239	304
NGPP	211	351	614
3 - 1 Cluster	308	483	816
1 - 1 Cluster	328	514	841

Table 5.12: The capital cost savings for the clustering the capture plants instead of using lone plants

	Savings 3-1 cluster [$ MM]	
	withouth comp	with comp
small	41	130
medium	57	160
Large	49	166
	Savings 1-1 cluster [$ MM]	
small	14.5	66
medium	14.3	75
Large	5.7	77

The cost of all facilities are shown in table 5.11. As table 5.12 shows, there are large savings for all sizes if the plants use the 3-1 cluster and use separate absorbers and share a large stripper for both with and without the CO_2 compression. The 1-1 cluster has a smaller saving, than the 3-1 but it is large enough to be significant. There seems to be no savings less relative savings as the sizes increase. this is partly due to how the cost calculations are set up. The equipment gets cheaper relative to how much it produces, the larger it gets. This has diminishing returns as the equipment size is increased. The large NGPP and cement facility probably have all ready gained all the cost savings in terms of up scaling the equipment, and there is no further gain in up scaling the equipment even more.

The running costs for the different faciliteies are shown in table 5.13. These can be used to see if the cluster configurations are more profitable than not clustering the plants. As table 5.14 shows, all the cluster options are more profitable than their lone counterparts, this is also reflected in the cost per tonne tabuleted in table 5.15.

Table 5.13: Running costs and income for the different plants

Facility				
Biogas	**cement**	**natgas**	**3-1 cluster**	**1-1 cluster**
Running cost without compression [$ MM]				
4.8	25	21	50	42
5.7	35	37	69	69
7.6	46	69	106	113
Running cost with compression [$ MM]				
6.3	33	26	60	52
7.7	45	45	85	85
19	59	82	131	136
Income normal tax [$ MM]				
1.4	28	16	45	44
2.8	42	32	76	74
5.6	56	62	124	119

Table 5.14: Yearly cost saving for the cluster configurations

	savings 3-1 [$ MM/yearly]	
	without comp	with comp
small	1.2	4.3
medium	9.1	12.9
Large	17	30
	savings 1-1 [$ MM/yearly]	
small	4.3	6.1
medium	3.8	5.5
Large	3.3	5.7

Cost of the pipelines are shown in table 5.16. Specifications for the pipe simulations were discussed in chapter 2.11. The solvent pipe will generally be twice as expensive as the CO_2 pipe. If the pipe is laid in difficult terrain or populated land, this price difference will decrease substantially[50].

To validate the pipeline prices, the price of the CO_2 pipeline was compared to prices for natural gas pipelines. Parker has collected data from 893 pipeline projects and presents

Table 5.15: Capture cost for the different facilities

Capture cost [$/tCO2]				
Biogas	**cement**	**natgas**	**3-1 cluster**	**1-1 cluster**
289	69	96	79	70
175	64	85	66	69
215	62	78	62	68

Table 5.16: Price for pipelines for the different facilities

Pipe	**Size**	**Biogas** [$ K/km]	**Cement** [$ K/km]	**NGPP** [$ K/km]	**3-1 Cluster** [$ K/km]	**1-1 Cluster** [$ K/km]
Flue	S	486	905	3,385	-	-
	M	585	1,675	4,153	-	-
	L	605	2,495	4,416	-	-
MEA	S	994	2,071	1,952	3,818	-
	M	1,162	2,918	2,442	5,791	-
	L	1,162	4,213	4,213	5,791	-
CO2	S	332	645	645	515	645
	M	332	825	515	825	825
	L	411	908	825	908	908

the average cost for the pipelines based on the NPS[51]. As both natural gas and CO_2 pipelines use high pressure, this was the most logical price to compare. The Average deviation for the cost is 35% and the absolute average deviation for the pipes are 23%. The deviations are presented graphically in figure 5.2. As pipelines will have very different cost based on the location of the pipeline, the overestimation up to 60% mean the cost estimation are well within the useful range.

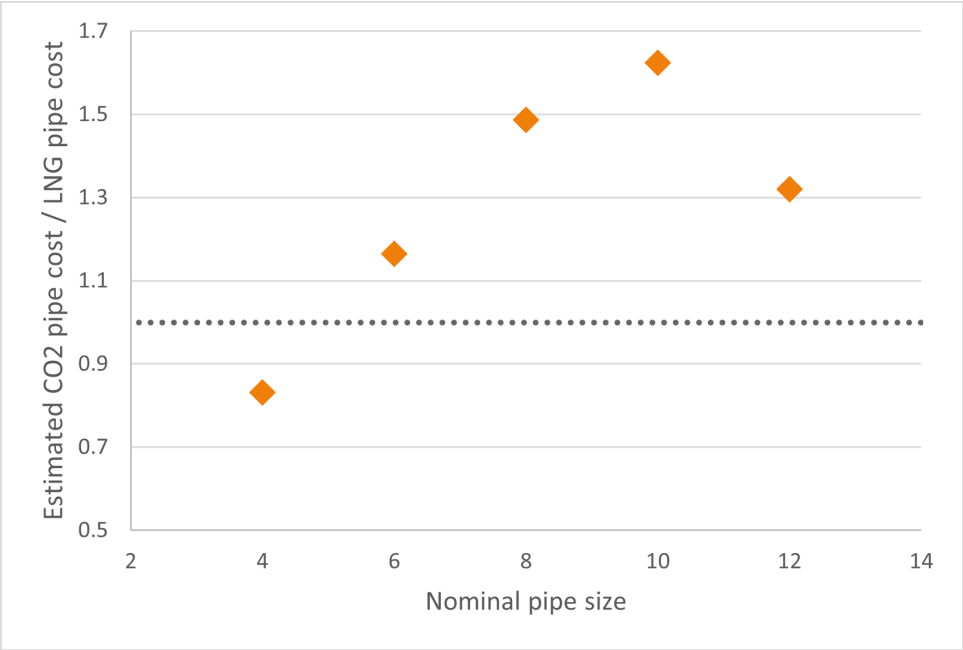

Figure 5.2: Estimated CO_2price divided by the average LNG pipe cost for same size

5.2.1 Sensitivity analysis

Sensetivity studies has been done to see the impact of CO_2 tax price increase, and cost of energy. This chapter presents results from the medium CO_2 plant. The other configurations have different numbers but the trends are similar to all plants.

CO_2tax The Norwegian tax for CO_2 emissions are today at 590 nok or aproximatly 59 dollars per tonne of CO_2[31]. As a part of Norway's climate plan, the tax will gradually be increased to 2000 nok per tonne in 2030[32]. To observe this impact the cash flow is examined with todays CO_2 tax, a tax of 100 dollars per tonne and the 2030 price of 200 dollars per tonne. As figure 5.3 shows the plant needs an increase in tax to have a positive cash flow and pay back the initial investment. With a carbon tax of 200 dollars per tonne the plant has a payback time of only 2 years, which means the plant could be seen as an investment opportunity and turn a profit for private investors.

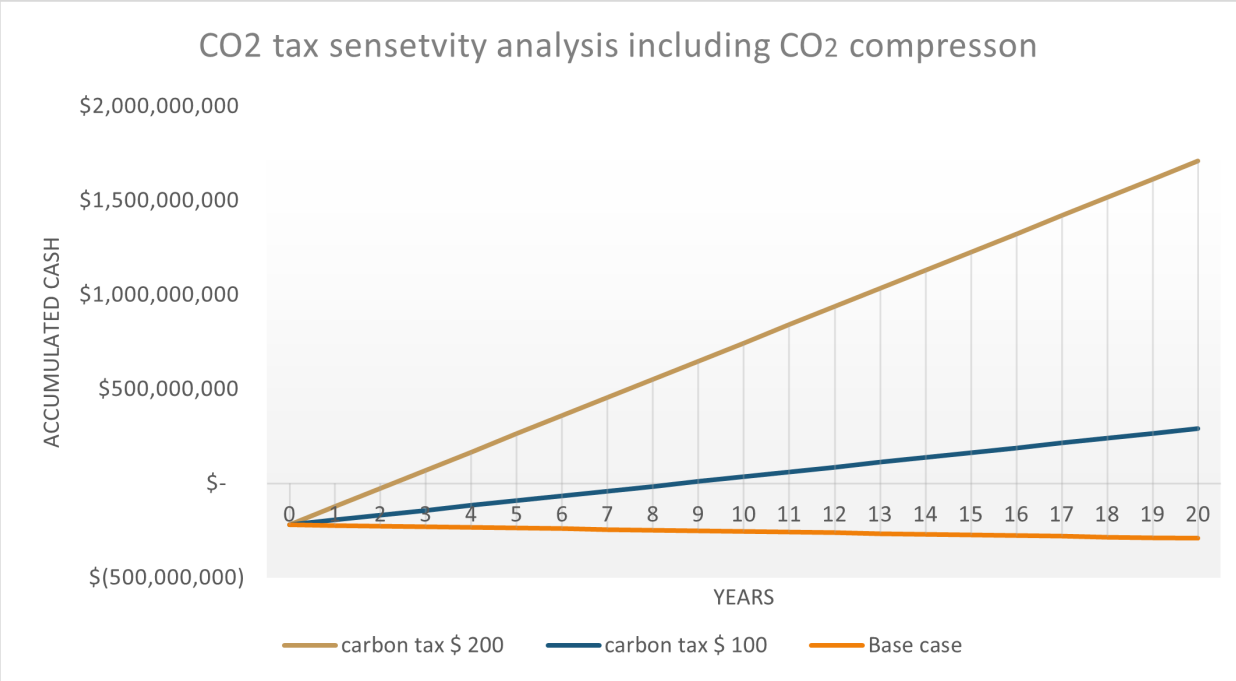

Figure 5.3: Sensitivity analysis using simple cash flow for the medium cement plant with varying CO_2 taxes

The see the impact of electricity prices and steam availability, steam has been set at 120% cost and 50% cost. 120% cost models an increase in electricity prices, which woul mean the steam price would also be higher, or for a NGPP, the penalty of lowering the electricity output to heat the reboiler would be higher. The cash flow is shown in figure 5.4. From this it can be observed that if the steam price is halved, the plant will have a positive cash flow. If the steam price is increased the plant will have operate at a greater loss. If the CO_2 tax is at 200 dollar per tonne, the plant will be profitable even with increased energy costs.

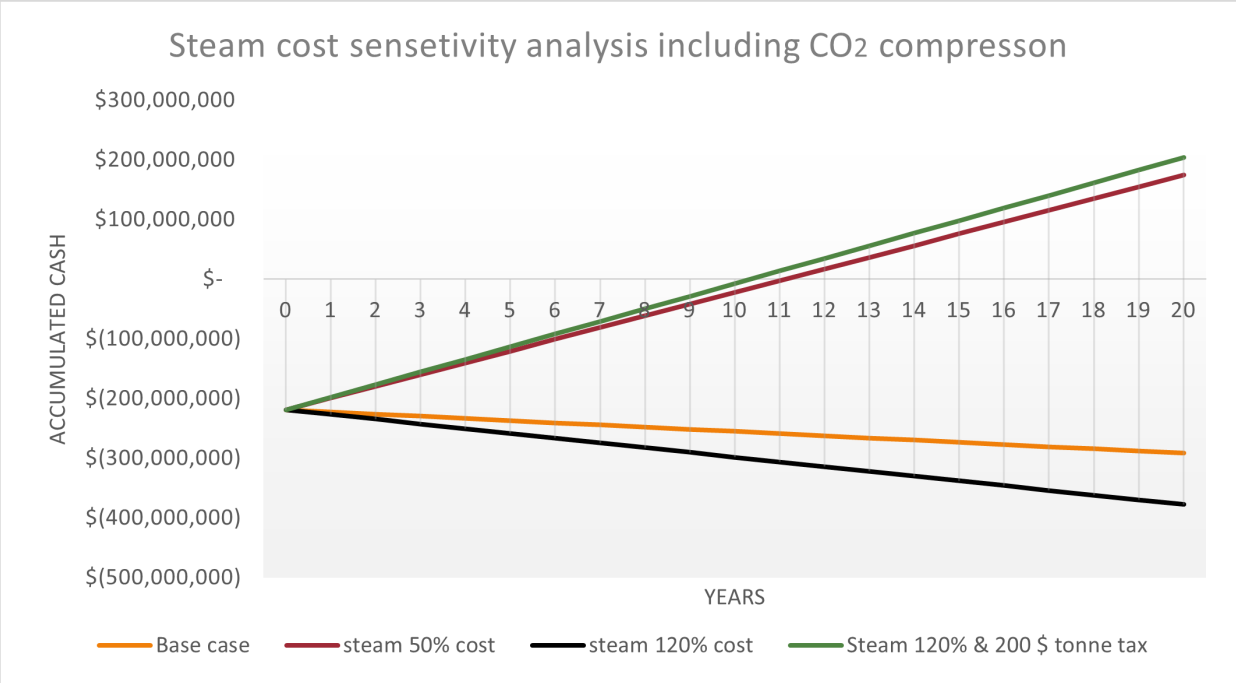

Figure 5.4: Sensitivity analysis using simple cash flow for the medium cement plant with varying steam orices

5.3 Example cases

To better get the Idea of the results presented, two example cases is evaluated in this chapter. the first is example is with a natural gas plant is situated 10 km from a biogas facility, 10 km from a cement plant, and 10 km from a port that ships the CO_2. This is illustrated in figure 5.5. Two configurations are suggested as an example of the costs for using the clusters. The first configuration called configuration 1A and pictured in figure 5.6. It will have an absorber and stripper on each plant, totaling 3 absorbers and 3 strippers. The CO_2 will be compressed to 20 bar in the cement and biogas plant, to then be transported via pipe to the NGPP. At the NGPP a CO_2 compression facility will compress all the CO_2 to 150 bar and pumped to the shipping port for offshore transport.

For configuration 1B pictured 5.7 the cement and biogas plant will be equipped with an absorber and the NGPP will be equipped with an absorber, stripper and a CO_2 compression system. This configuration uses 3 absorbers and 1 stripper, called 3-1 cluster. The solvent will be pumped back and forth from the absorbers on the biogas and cement plant along a MEA pipeline. The capital cost and running costs are presented in table 5.17. Using configuration B, the 3-1 cluster offer huge savings in both capital cost and running costs. The savings for using the 3-1 cluster is probably exaggerated by the fact that the strippers used in this thesis is much larger than strippers used in other works, as discussed previously in chapter 5.1.2. The running cost is also considerably better in option B. This is gain is also slightly inflated due to the biogas plant being too small to be profitable, and having a high running cost compared

to the CO_2 captured. If the running costs for the biogas plant is omitted the running costs are at 90 $ MM, which means the 3-1 cluster is still much more cost efficient even without the biogas cost. The pipeline costs in this are also for a best case scenario, meaning it goes through unpopulated land with no geological difficulties.

Table 5.17: Capital cost and running cost for the two configurations

Cost	Config. 1A [$ MM]	Config. 1B [$ MM]
Capital cost	610	532
Running cost	96	85

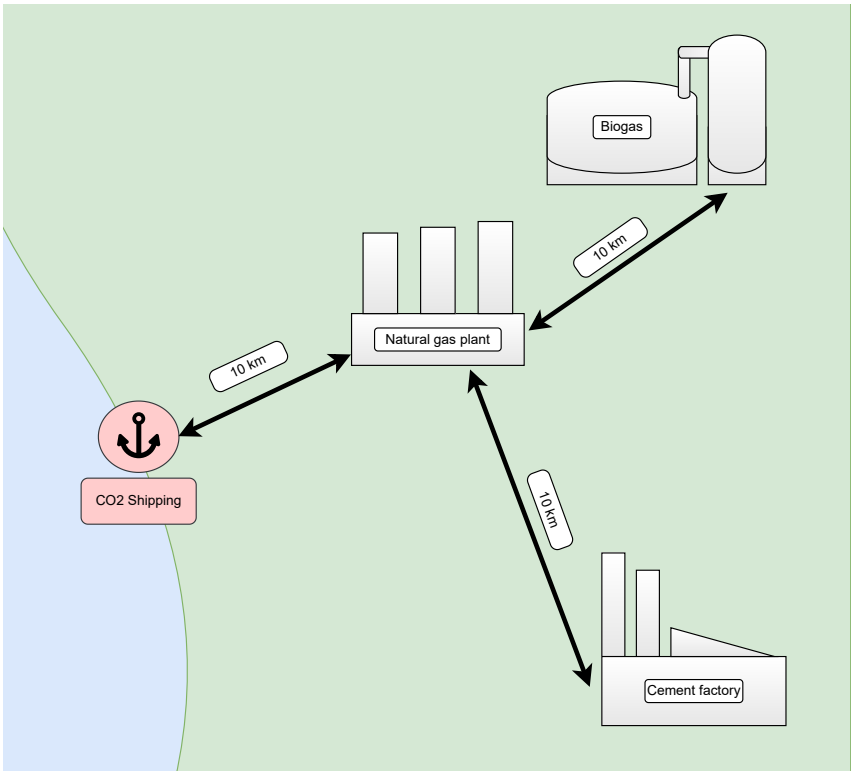

Figure 5.5: Example case 1 for equipping different plants with CO_2 capture

The second example will be identical to the one presented above, except it will not have a biogas plant as shown in figure 5.8. The two configurations for this example will be either: Configuration 2A, each plant with their own absorber, and pumping CO_2 at 20 bar from the cement plant to the NGPP. At the NGPP all the CO_2 is pressurised to 150 bar and sent to the port as shwon in figure 5.9. Configuration 2B will use the 1-1 cluster and pump the flue gas from the cement factory and treat all the gas at the NGPP. From here the gas will also be pressurised to 150 bar and pumped to the shipping port as shown in figure 5.10. The cost the two configurations are shown in table 5.18. configuration 2 B clustering the absorber and stripper to one unit have a lower capital cost, this small gain in lower capital cost is far outweighed in the increased running cost of the plant. This is due to the high electricity cost of pumping the gas through flue

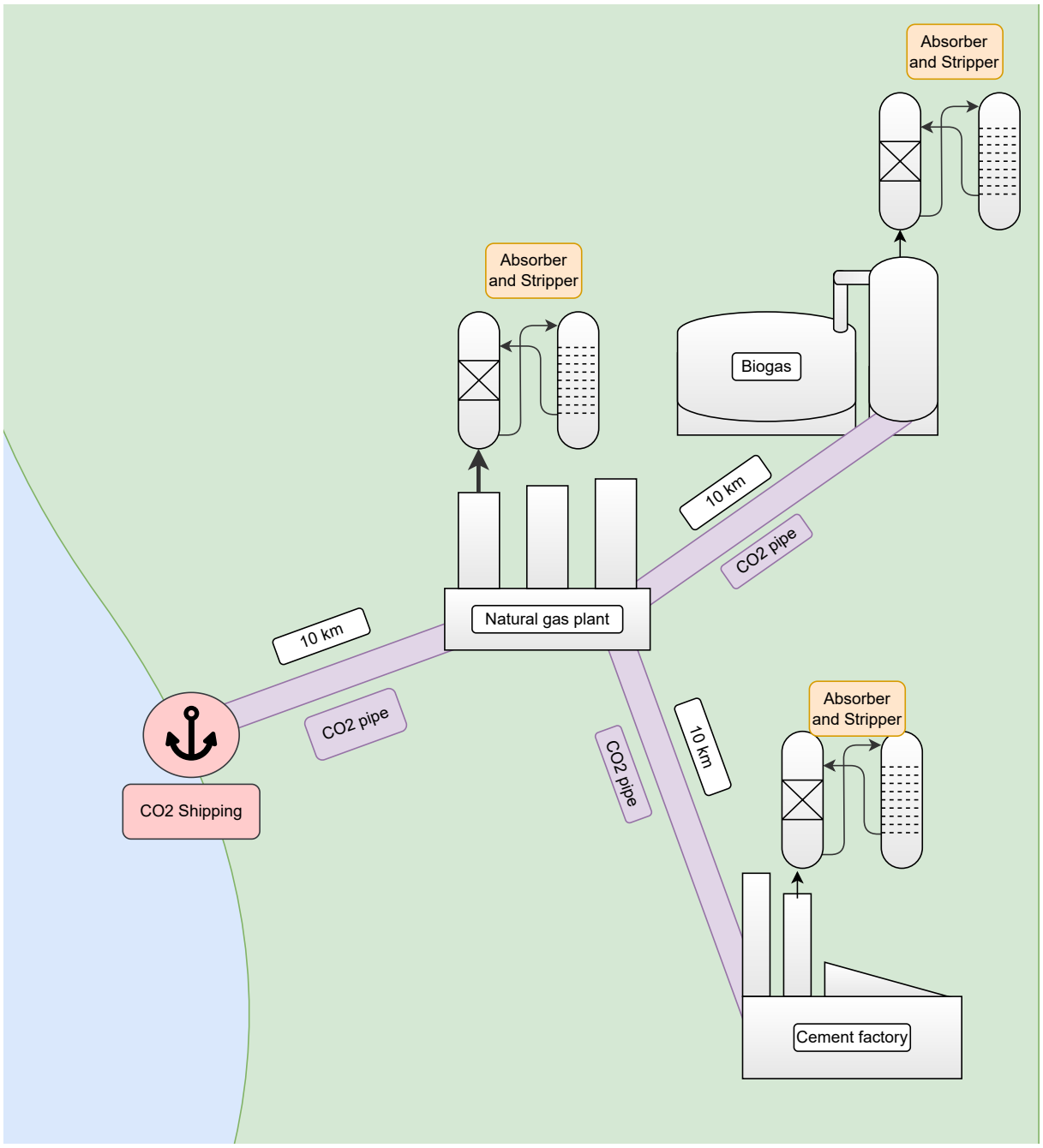

Figure 5.6: Configuration A for CO_2 capture, 3 absorbers and 3 strippers with CO_2 pipeline

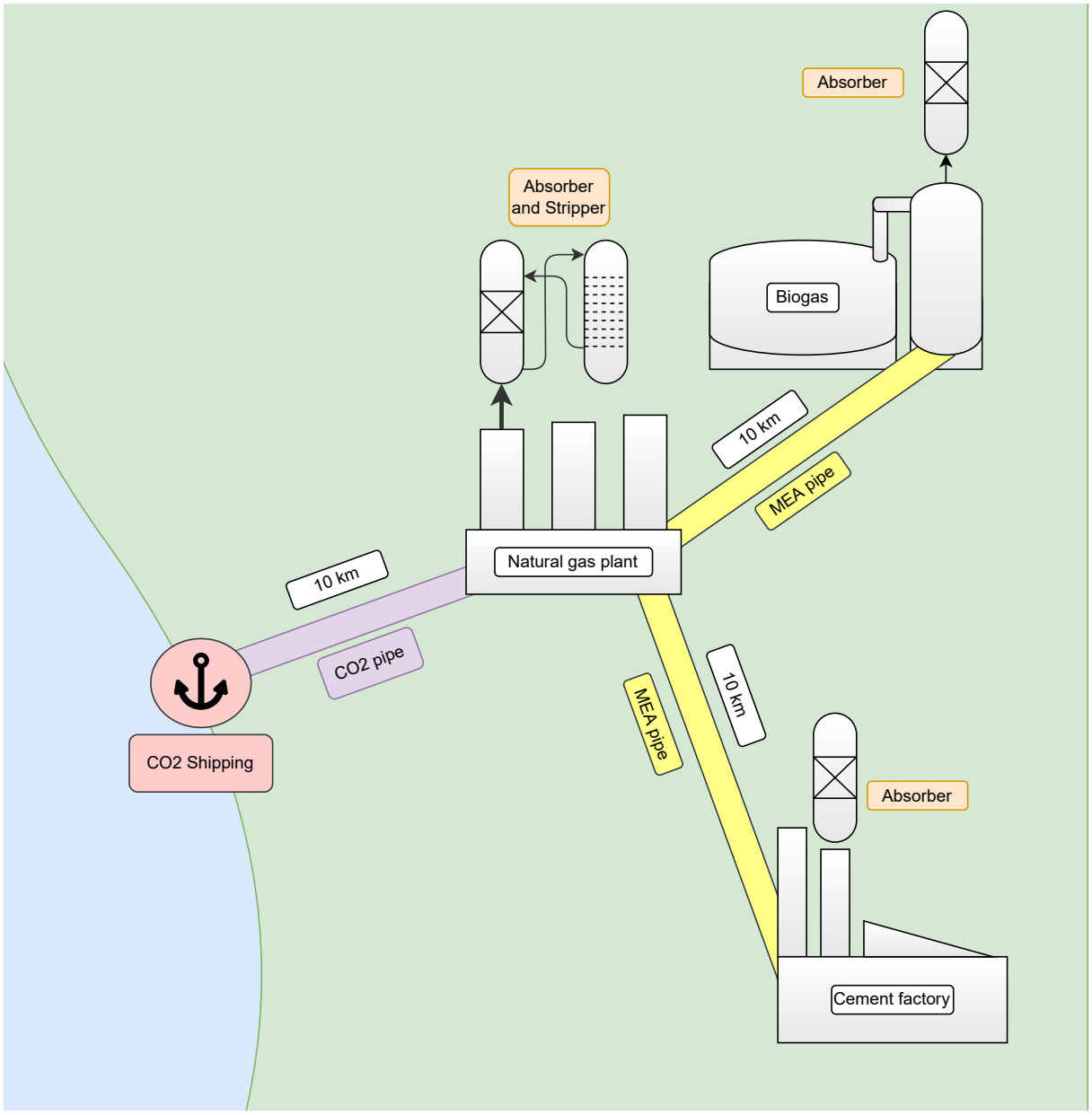

Figure 5.7: Configuration B for CO_2 capture, 3 absorbers and 1 stripper with MEA pipelines

pipelines. The break even point for operating costs is at 4 km. This means that if the cement plant is closer than 4 km to the NGPP, it is cheaper to use option B.

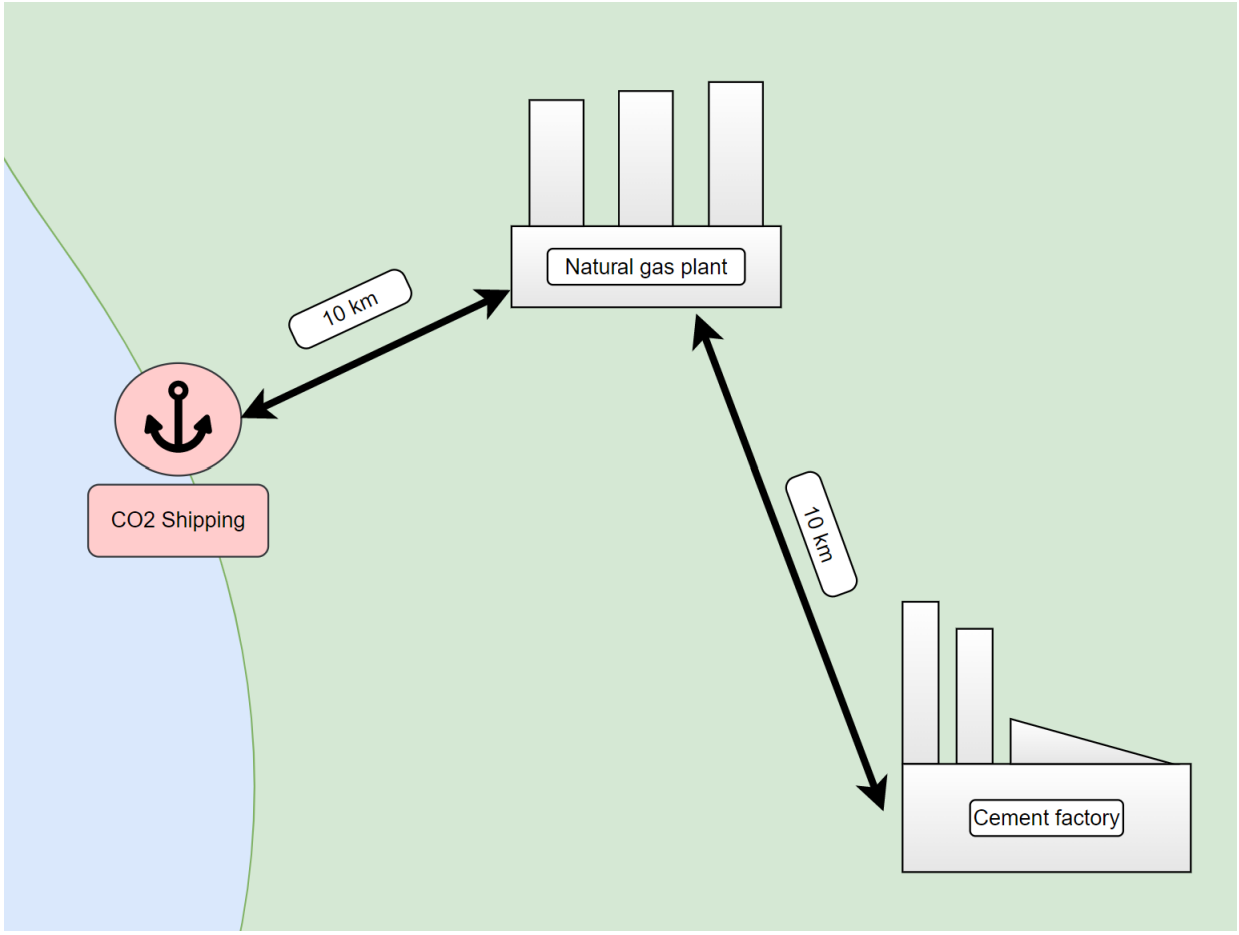

Figure 5.8: Example case 2 for equipping different plants with CO_2 capture

Table 5.18: Capital cost and running cost for the two configurations

	Config. 2A [$ MM]	**Config. 2B [$ MM]**
Capital cost	578	540
Running cost	90	95

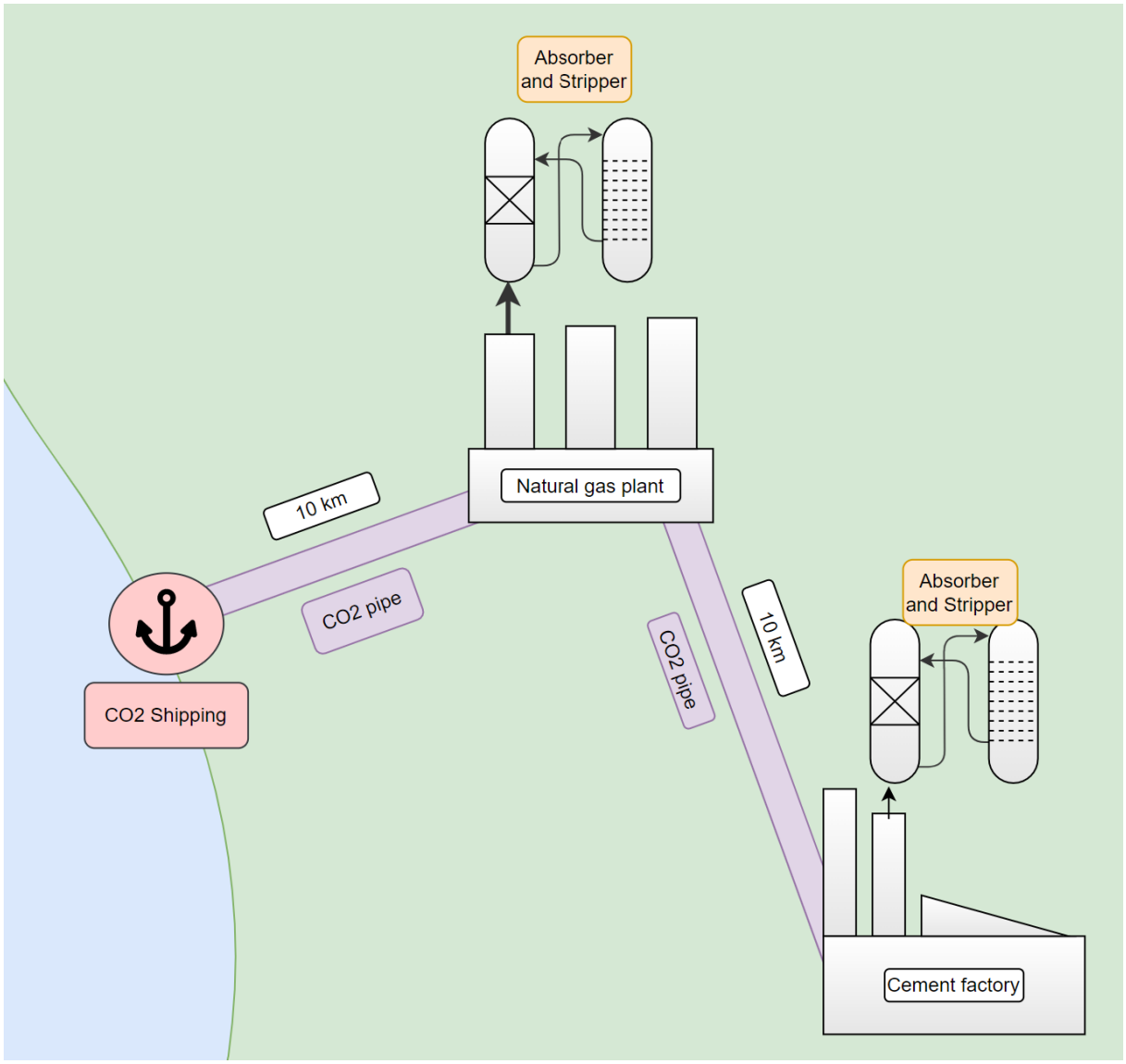

Figure 5.9: Configuration 2A for CO_2 capture, 2 absorbers and 2 strippers with CO_2 pipelines

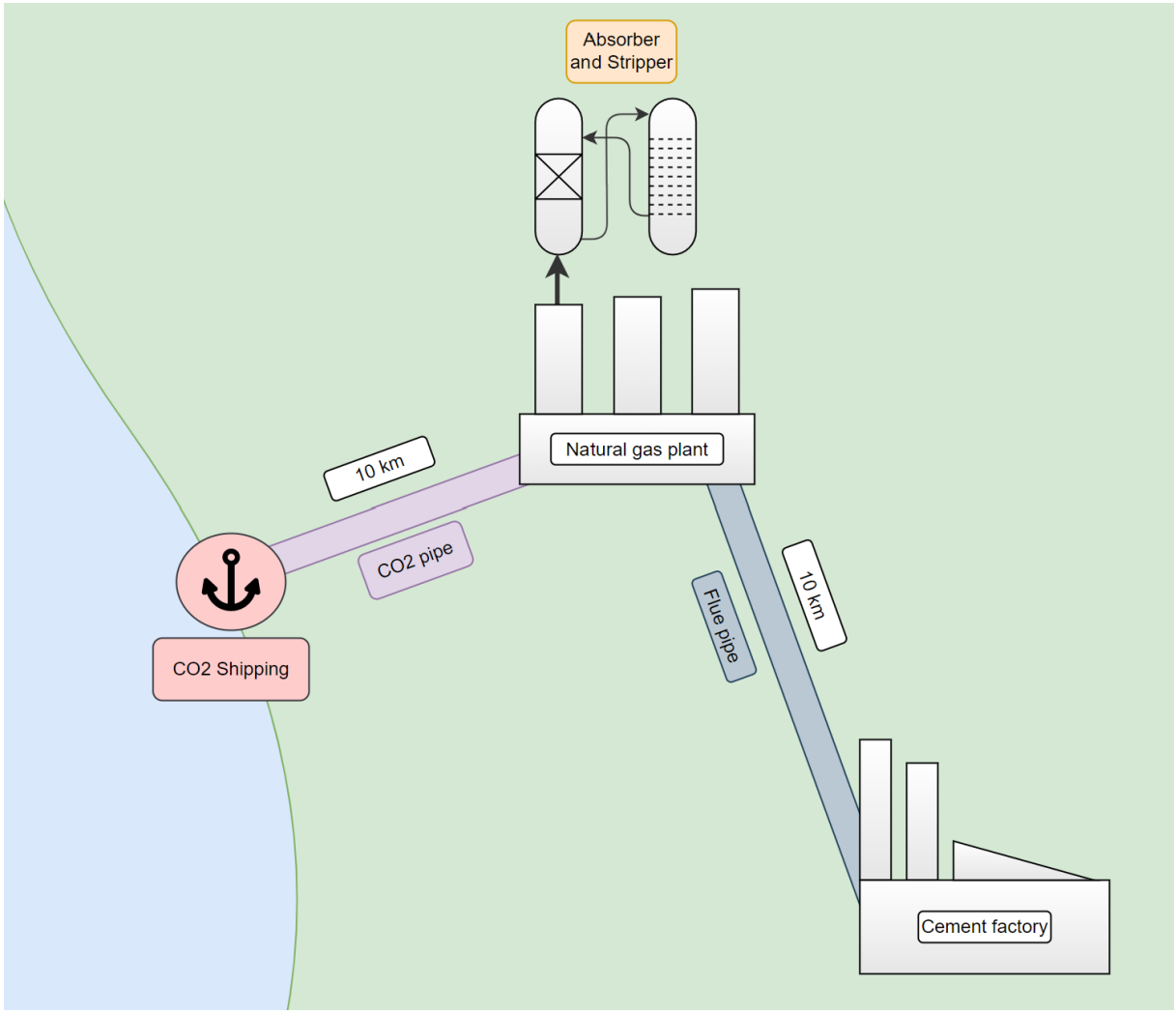

Figure 5.10: Configuration 2B for CO_2 capture, 1 absorber and 1 stripper with flue gas pipelines

6 Conclusion

This thesis has found that clustering CO_2 facilities together can give a lower capture cost. There is some potential saving in pumping flue gas from facilities to one central large absorber and stripper. There is a large potential gain in clustering CO_2 capture plants with separate absorbers for each facility and with one central stripper. Pipeline systems pumping MEA solvents can be set up for approximately twice the price of CO_2 pipes, with very low pumping costs. Pumping the flue gas has such a high electricity usage that the pipelines can not travel far before all the savings using the 1-1 cluster is lost.

References

[1] United nations. Climate change 'biggest threat modern humans have ever faced', worldrenowned naturalist tells security council, calls for greater global cooperation, 2021.

[2] United nations. Noaa national centers for environmental information, 2022. URL https://www.ncdc.noaa.gov/cag/.

[3] A Connors V Zhai, P Pirani. Climate change 2021: The physical science basis. 2021. URL https://www.ipcc.ch/report/ar6/wg1/downloads/report/IPCC_AR6_WGI_Full_Report.pdf.

[4] IEA. Energy technology perspectives 2015. *IEA*, 2015. URL https://www.iea.org/reports/energy-technology-perspectives-2015.

[5] M Tignor Pörtner, DC Roberts. Climate change 2022: Impacts, adaptation, and vulnerability. contribution of working group ii to the sixth assessment report of the intergovernmental panel on climate change, 2022. URL https://www.ipcc.ch/report/ar6/wg1/downloads/report/IPCC_AR6_WGI_Full_Report.pdf.

[6] Yue Zhang, Darshan Sachde, Eric Chen, and Gary Rochelle. Modeling of absorber pilot plant performance for co2 capture with aqueous piperazine. *International Journal of Greenhouse Gas Control*, 64:300–313, 2017. ISSN 1750-5836. doi: https://doi.org/10.1016/j.ijggc.2017.08.004. URL https://www.sciencedirect.com/science/article/pii/S1750583617303985.

[7] Johan Fagerlund, Ron Zevenhoven, Jørgen Thomassen, Marius Tednes, Farhang Abdollahi, Laurent Thomas, Claus Jørgen Nielsen, Tomas Mikoviny, Armin Wisthaler, Liang Zhu, Chet Biliyok, and Andrey Zhurkin. Performance of an amine-based co2 capture pilot plant at the fortum oslo varme waste to energy plant in oslo, norway. *International Journal of Greenhouse Gas Control*, 106:103242, 2021. ISSN 1750-5836. doi: https://doi.org/10.1016/j.ijggc.2020.103242. URL https://www.sciencedirect.com/science/article/pii/S1750583620306678.

[8] Marcin Stec, Adam Tatarczuk, Lucyna Więcław-Solny, Aleksander Krótki, Tomasz Spietz, Andrzej Wilk, and Dariusz Śpiewak. Demonstration of a post-combustion carbon capture pilot plant using amine-based solvents at the łaziska power plant in poland. *Clean Technologies and Environmental Policy*, 18(1):151–160, June 2015. doi: 10.1007/s10098-015-1001-2. URL https://doi.org/10.1007/s10098-015-1001-2.

[9] G.T. Rochelle. 3 - conventional amine scrubbing for co2 capture. In Paul H.M. Feron, editor, *Absorption-Based Post-combustion Capture of Carbon Dioxide*, pages

35–67. Woodhead Publishing, 2016. ISBN 978-0-08-100514-9. doi: https://doi.org/10.1016/B978-0-08-100514-9.00003-2. URL https://www.sciencedirect.com/science/article/pii/B9780081005149000032.

[10] G.S. Booras and S.C. Smelser. An engineering and economic evaluation of co2 removal from fossil-fuel-fired power plants. *Energy*, 16(11):1295–1305, 1991. ISSN 0360-5442. doi: https://doi.org/10.1016/0360-5442(91)90003-5. URL https://www.sciencedirect.com/science/article/pii/0360544291900035.

[11] Anand B. Rao and Edward S. Rubin. A technical, economic, and environmental assessment of amine-based co2 capture technology for power plant greenhouse gas control. *Environmental Science & Technology*, 36(20):4467–4475, 2002. doi: 10.1021/es0158861. URL https://doi.org/10.1021/es0158861. PMID: 12387425.

[12] Jiri van Straelen, Frank Geuzebroek, Nicholas Goodchild, Georgios Protopapas, and Liam Mahony. Co2 capture for refineries, a practical approach. *International Journal of Greenhouse Gas Control*, 4(2):316–320, 2010. ISSN 1750-5836. doi: https://doi.org/10.1016/j.ijggc.2009.09.022. URL https://www.sciencedirect.com/science/article/pii/S175058360900111X. The Ninth International Conference on Greenhouse Gas Control Technologies.

[13] Adina Bosoaga, Ondrej Masek, and John E. Oakey. Co2 capture technologies for cement industry. *Energy Procedia*, 1(1):133–140, 2009. ISSN 1876-6102. doi: https://doi.org/10.1016/j.egypro.2009.01.020. URL https://www.sciencedirect.com/science/article/pii/S1876610209000216. Greenhouse Gas Control Technologies 9.

[14] Ernst Worrell, Lynn Price, Nathan Martin, Chris Hendriks, and Leticia Ozawa Meida. Carbon dioxide emissions from the global cement industry. *Annual Review of Energy and the Environment*, 26(1):303–329, 2001. doi: 10.1146/annurev.energy.26.1.303. URL https://doi.org/10.1146/annurev.energy.26.1.303.

[15] Shome A. Goswami R., Chattopadhyay P. An overview of physico-chemical mechanisms of biogas production by microbial communities: a step towards sustainable waste management. *3 Biotech*, 2016. URL https://doi.org/10.1007/s13205-016-0395-9.

[16] Hannah Ritchie and Max Roser. Energy. *Our World in Data*, 2020. https://ourworldindata.org/energy.

[17] Gary T. Rochelle. Amine scrubbing for co₂ capture. *Science*, 325 (5948):1652–1654, 2009. doi: 10.1126/science.1176731. URL https://www.science.org/doi/abs/10.1126/science.1176731.

[18] Jason Davis and Gary Rochelle. Thermal degradation of monoethanolamine at stripper conditions. *Energy Procedia*, 1(1):327–333, 2009. ISSN 1876-6102. doi: https://doi.org/10.1016/j.egypro.2009.01.045. URL https://www.sciencedirect.com/science/article/pii/S1876610209000460. Greenhouse Gas Control Technologies 9.

[19] Bihong Lv, Bingsong Guo, Zuoming Zhou, and Guohua Jing. Mechanisms of co2 capture into monoethanolamine solution with different co2 loading during the absorption/desorption processes. *Environmental Science & Technology*, 49(17):10728–10735, 2015. doi: 10.1021/acs.est.5b02356. URL https://doi.org/10.1021/acs.est.5b02356. PMID: 26236921.

[20] Gavin Towler and Ray Sinnott. Chapter 7 - capital cost estimating. In Gavin Towler and Ray Sinnott, editors, *Chemical Engineering Design (Second Edition)*, pages 307–354. Butterworth-Heinemann, Boston, second edition edition, 2013. ISBN 978-0-08-096659-5. doi: https://doi.org/10.1016/B978-0-08-096659-5.00007-9. URL https://www.sciencedirect.com/science/article/pii/B9780080966595000079.

[21] Gavin Towler and Ray Sinnott. Chapter 14 - design of pressure vessels. In Gavin Towler and Ray Sinnott, editors, *Chemical Engineering Design (Second Edition)*, pages 563–629. Butterworth-Heinemann, Boston, second edition edition, 2013. ISBN 978-0-08-096659-5. doi: https://doi.org/10.1016/B978-0-08-096659-5.00014-6. URL https://www.sciencedirect.com/science/article/pii/B9780080966595000146.

[22] Hassan Ali, Nils Henrik Eldrup, Fredrik Normann, Ragnhild Skagestad, and Lars Erik Øi. Cost estimation of co2 absorption plants for co2 mitigation – method and assumptions. *International Journal of Greenhouse Gas Control*, 88:10–23, 2019. ISSN 1750-5836. doi: https://doi.org/10.1016/j.ijggc.2019.05.028. URL https://www.sciencedirect.com/science/article/pii/S1750583618309332.

[23] R. Dutta. *Fundamentals of Biochemical Engineering*. Springer, 2010. ISBN 9783642096747. URL https://books.google.no/books?id=zghUcgAACAAJ.

[24] Electricity price statistics, 2022. URL https://ec.europa.eu/eurostat/statistics-explained/index.php?title=Electricity_price_statistics#Electricity_prices_for_household_consumers.

[25] Eu sanctions against russia explained, 2022. URL https://europa.eu/!xjjknT.

[26] Chikezie Nwaoha, Martin Beaulieu, Paitoon Tontiwachwuthikul, and Mark D. Gibson. Techno-economic analysis of co2 capture from a 1.2 million mtpa cement plant using amp-pz-mea blend. *International Journal of Greenhouse Gas Control*, 78:400–

412, 2018. ISSN 1750-5836. doi: https://doi.org/10.1016/j.ijggc.2018.07.015. URL https://www.sciencedirect.com/science/article/pii/S1750583618303566.

[27] Solomon Aforkoghene Aromada, Nils Henrik Eldrup, and Lars Erik Øi. Capital cost estimation of co2 capture plant using enhanced detailed factor (edf) method: Installation factors and plant construction characteristic factors. *International Journal of Greenhouse Gas Control*, 110:103394, 2021. ISSN 1750-5836. doi: https://doi.org/10.1016/j.ijggc.2021.103394. URL https://www.sciencedirect.com/science/article/pii/S1750583621001468.

[28] In the u.s. and around the world, inflation is high and getting higher, 2022. URL https://www.pewresearch.org/fact-tank/2022/06/15/in-the-u-s-and-around-the-world-inflation-is-high-and-getting-higher/#:~:text=According%20to%20the%20latest%20report,by%20the%20consumer%20price%20index.

[29] GERRARD A M ALKHAYAT W A. Estimating manning levels for process plants. *About Transactions of the American Association of Cost Engineers. Annual Meeting*, 28:I.2.1–I.2.4, 1984. ISSN 0065-7158. URL https://jglobal.jst.go.jp/en/detail?JGLOBAL_ID=200902094600205443.

[30] Karbonfangst ved norcem brevik, 2022. URL https://www.norcem.no/no/CCS_Brevik.

[31] finansdepartementet. avgiftsatser 2022, 2022. URL https://www.regjeringen.no/no/tema/okonomi-og-budsjett/skatter-og-avgifter/avgiftssatser-2022/id2873933/.

[32] finansdepartementet. Oversikt over alle regjeringa vil-punkta i meldinga, 2022. URL https://www.regjeringen.no/contentassets/202fec60ac844d4ca7d53d65b6b9ac9c/alle-regjeringa-vil-punkt-i-meldinga.pdf.

[33] Gavin Towler and Ray Sinnott. Chapter 5 - instrumentation and process control. In Gavin Towler and Ray Sinnott, editors, *Chemical Engineering Design (Second Edition)*, pages 251–277. Butterworth-Heinemann, Boston, second edition edition, 2013. ISBN 978-0-08-096659-5. doi: https://doi.org/10.1016/B978-0-08-096659-5.00005-5. URL https://www.sciencedirect.com/science/article/pii/B9780080966595000055.

[34] Fang-Yuan Jou, Alan E. Mather, and Frederick D. Otto. The solubility of co2 in a 30 mass percent monoethanolamine solution. *The Canadian Journal of Chemical En-*

gineering, 73(1):140–147, 1995. doi: https://doi.org/10.1002/cjce.5450730116. URL https://onlinelibrary.wiley.com/doi/abs/10.1002/cjce.5450730116.

[35] Finn Andrew Tobiesen, Hallvard F. Svendsen, and Olav Juliussen. Experimental validation of a rigorous absorber model for co2 postcombustion capture. *AIChE Journal*, 53(4):846–865, 2007. doi: https://doi.org/10.1002/aic.11133. URL https://aiche.onlinelibrary.wiley.com/doi/abs/10.1002/aic.11133.

[36] Diego Pinto, Hanna Knuutila, Georgios Fytianos, Geir Haugen, Thor Mejdell, and Hallvard Svendsen. Co2 post combustion capture with a phase change solvent. pilot plant campaign. *International Journal of Greenhouse Gas Control*, 31:153–164, 12 2014. doi: 10.1016/j.ijggc.2014.10.007.

[37] Trine Witzøe. Simulation of pilot data with aspen plus. 2015.

[38] Finn Tobiesen, Olav Juliussen, and Hallvard Svendsen. Experimental validation of a rigorous desorber model for co 2 post-combustion capture. *Chemical Engineering Science - CHEM ENG SCI*, 63:2641–2656, 05 2008. doi: 10.1016/j.ces.2008.02.011.

[39] Arthur WELLINGER Margareta PERSSON, Owe JÖNSSON. Biogas upgrading to vehicle fuel standards and grid injection. *IEA bioenergy*, 2007. URL hhttps://www.ieabioenergy.com/blog/publications/biogas-upgrading-to-vehicle-fuel-standards-and-grid-injection/.

[40] Power blocks in natural gas-fired combined-cycle plants are getting bigger, 2022. URL https://www.eia.gov/todayinenergy/detail.php?id=38312#:~:text=Since%202014%2C%20the%20average%20size,of%20820%20MW%20in%202017.

[41] How many cement plants are producing in the usa 2020?, 2022. URL https://datis-inc.com/blog/how-many-cement-plants-are-producing-in-the-usa-2020/#The_Largest_Cement_Plants_in_the_USA-Top_10.

[42] R. Steeneveldt, B. Berger, and T.A. Torp. Co2 capture and storage: Closing the knowing–doing gap. *Chemical Engineering Research and Design*, 84(9):739–763, 2006. ISSN 0263-8762. doi: https://doi.org/10.1205/cherd05049. URL https://www.sciencedirect.com/science/article/pii/S0263876206729562. Carbon Capture and Storage.

[43] Lanyu Gao, Mengxiang Fang, Hailong Li, and Jens Hetland. Cost analysis of co2 transportation: Case study in china. *Energy Procedia*, 4:5974–5981, 2011. ISSN 1876-6102. doi: https://doi.org/10.1016/j.egypro.2011.02.600. URL https:

//www.sciencedirect.com/science/article/pii/S1876610211008794. 10th International Conference on Greenhouse Gas Control Technologies.

[44] Chechet Biliyok, Roberto Canepa, Meihong Wang, and Hoi Yeung. Techno-economic analysis of a natural gas combined cycle power plant with co2 capture. In Andrzej Kraslawski and Ilkka Turunen, editors, *23rd European Symposium on Computer Aided Process Engineering*, volume 32 of *Computer Aided Chemical Engineering*, pages 187–192. Elsevier, 2013. doi: https://doi.org/10.1016/B978-0-444-63234-0.50032-4. URL https://www.sciencedirect.com/science/article/pii/B9780444632340500324.

[45] Kwangsu Park and Lars Øi. Optimization of gas velocity and pressure drop in co2 absorption column, 09 2017.

[46] Column analysis in aspen plus® and aspen hysys® :validation with experimental and plant data, 2018. URL https://www.aspentech.com/en/resources/white-papers/column-analysis-in-aspen-plus-and-aspen-hysys---validation-with-experimental-and-

[47] Silje Hjelmaas, Erlend Storheim, Nina Enaasen Flø, Eva Svela Thorjussen, Anne Kolstad Morken, Leila Faramarzi, Thomas de Cazenove, and Espen Steinseth Hamborg. Results from mea amine plant corrosion processes at the co2 technology centre mongstad. *Energy Procedia*, 114:1166–1178, 2017. ISSN 1876-6102. doi: https://doi.org/10.1016/j.egypro.2017.03.1280. URL https://www.sciencedirect.com/science/article/pii/S1876610217314613. 13th International Conference on Greenhouse Gas Control Technologies, GHGT-13, 14-18 November 2016, Lausanne, Switzerland.

[48] Norcem brevik, 2020. URL https://www.norcem.no/no/CCS_i_Brevik.

[49] Norcem brevik, 2021. URL https://e24.no/olje-og-energi/i/mrvQag/co-fangstanlegg-sprekker-med-naer-en-milliard.

[50] Le Li, Alexander K. Voice, Han Li, Omkar Namjoshi, Thu Nguyen, Yang Du, and Gary T. Rochelle. Amine blends using concentrated piperazine. *Energy Procedia*, 37:353–369, 2013. ISSN 1876-6102. doi: https://doi.org/10.1016/j.egypro.2013.05.121. URL https://www.sciencedirect.com/science/article/pii/S1876610213001318. GHGT-11 Proceedings of the 11th International Conference on Greenhouse Gas Control Technologies, 18-22 November 2012, Kyoto, Japan.

[51] Using natural gas transmission pipeline costs to estimate hydrogen pipeline costs, 2001. URL https://escholarship.org/content/qt2gk0j8kq/qt2gk0j8kq_noSplash_cfbe115e54fba9e62c107c7ac2f3ef17.pdf.

Appendix

A flowsheet modifications

Most of the units and streams in the flow sheet are done according to the flow sheet in figure bla bla. however several additions and modification were done to the flow sheet to aid convergence, these are presented and explained in this chapter

A.1 Solvent concentration and amount control

To manage the concentration and the amount of solvent used in the system, several options were tried to find the optial system. Many of the designs tried had issues regarding the convergence of the flowsheet, or the stability of the solvent compostion and ammount through multiple iterations.

The first design solution shown in figure A.1 had the recycle stream (COLDLEAN) from the stripper cooled, mixed with water from the water wash (FROMWW), a makeup stream (MU) consisting of water and MEA, and sent to the absorber. The makeup stream uses Aspen + balance equation, in which the make up streams composition and amount is calculated based on the amount of a component entering and leaving the system. In this instance the inlet stream were the flue gas and make up stream, and outlet streams were gas out of absorber and the co2 product from the stripper, as these were the streams water and MEA would loss of the system would oocour.

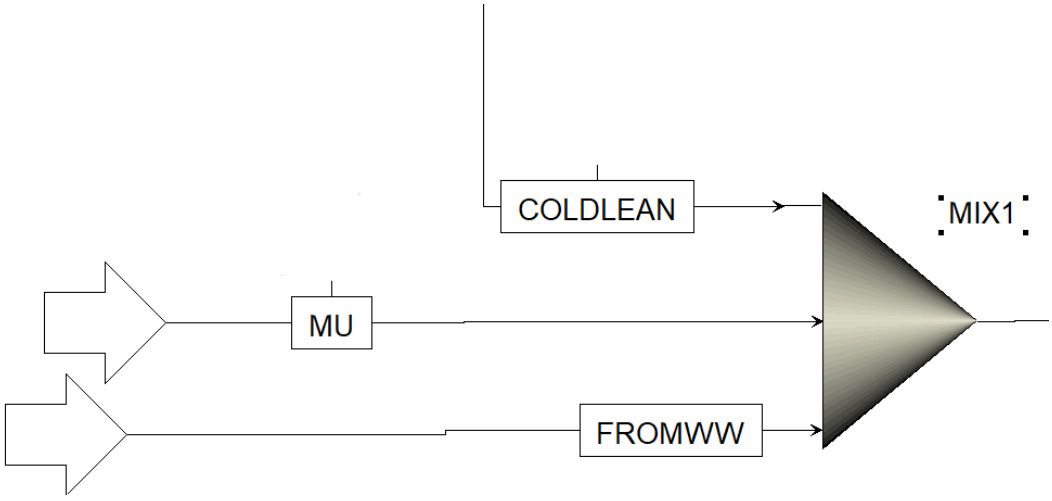

Figure A.1: first design

This solution was not very stable, as an error in the stripper or absorber would change the concentration and flow amount in the stream. With no system in place to continually fix the solvent amount or conenctration, using this design for SRD analysis would be highly impractical.

To set the concentration in the stream a design spec block was added to the system. This design block had the objective to control the concentration of MEA, and keep it constant at 30 weight% MEA. The design spec block controlled the stream MEACONC and chose the ammount of MEA in the stream to keep the concentration stable.

This solution was more stable, but had problems across several iterations of the flowsheet. The ammount of MEA in the stream would often gradually increase acros many iterations. at iteration 1 the stream would supply 1% of the systems water and MEA, but after 100 iterations this could go up to 20 %, giving possible errors in the results gathered from these simulations. The solution was not perfectly stable either, as the stream could not have negative mass flow. Meaning that if the concentration of the MEA was at 31 Weight%, and the MEACONC stream had no MEA flow, there was no way to lower the concentration. This design had also not addressed the control issue of solvent amount in the system

another solution to control the flow was to add a stream multiplying block with a calculator as in A.2. The calculator block would control the myliplying block to get the correct amount of solvent for each iteration. The idea was that if the stream was ie. to low, the calculator would myltiply with ie. 1.1, and the correct amount of selvent would flow thorugh the system, and when the solvent came back to the multiplier block, the stream would now have the correct amount of solvent, and the calculatior block would mulypling the stream with 1.0, not altering the stream in any way. this solution was not stabel enough, possibly due to the the calculator block oscilating betwen the solutin ie. 1.1 –> 0.9 –> 1.1.

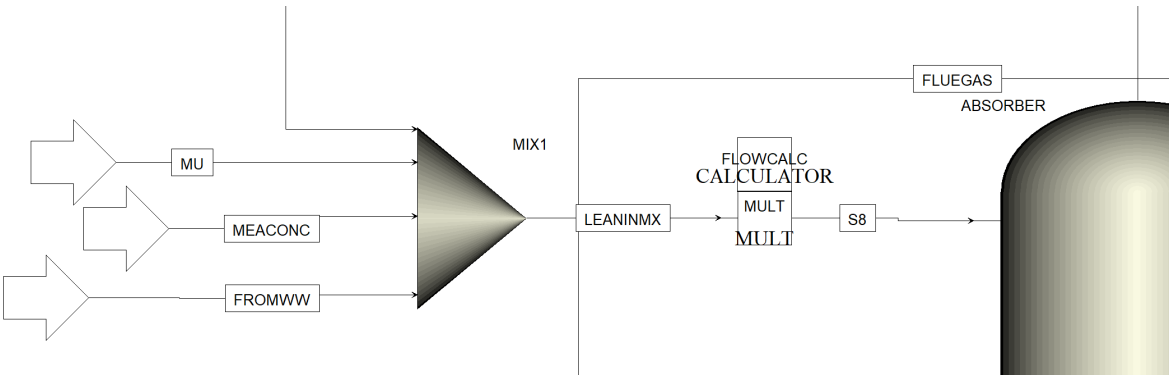

Figure A.2: Caption

Altering the amount of water from the water wash as a control option was also tried, but did not yield any better results than the other options.

A solution to this was to add a stream with approximately 10% of the systems total solvent flow in the first mixer, and remove aproxomatly 10 % of the solvent before entering the absorber. The amount removed would vary to keep the amount entering the absorber

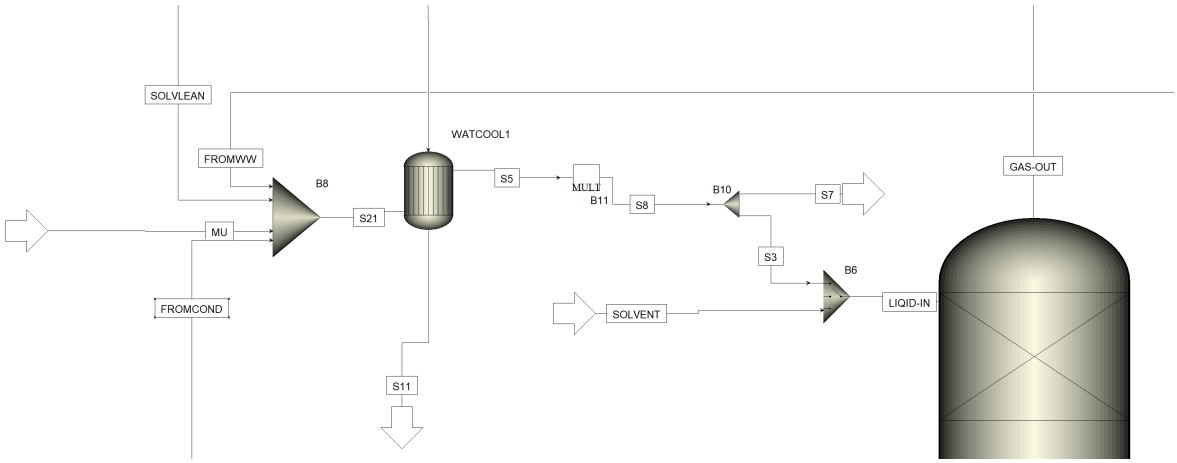

Figure A.3: Caption

constant. This stream (FRESHMEA) had the same MEA weight% and same CO_2 loading as the solvent in the system. This solution yielded the best stability and solvent control options of all the options mentioned so far. It made the entire system stable across many iterations, and was used for much of the prelimenary system investetgations. however, this soluton had the big disadvantage of making the calculations and results of the flowsheet suspect and not trust worthy.

The final design depicted in figure A.3, which all the simulations in this report uses is a design with a stream multiplier and a stream splitter, with no ongoing concentration control. The stream after the mixer is doubled, and then the necessary amount is removed to achieve the desired solvent amount. The concentration is set with the SOLVENT stream, and then the system is switched to the circulating stream. As this system proved very stable, the concentration would usually only change a significant amount at a very high number of flow sheet iterations, from 500 - 5000 iterations. And with the stream selector block, the correct solvent composition could be quickly regained by switching to the solvent stream for one iteration and switching back. This final design uses a heat exchanger to meassure the amount of cooling water necesary for the stream, and to size the system correctly. In this final design the condensed liquid from the stripper is sent directly from the condenser to the solvent mixer, the reasoning behind this is discussed in chapter A.3 below.

A.2 Pseudo water wash

To avoid emitting MEA into the atmosphere from the absorber, the top section of the absorber is equipped with a water wash. this water wash will absorb the MEA mist, and send some of the water in the water wash to the solvent. To model this a rad frac absorber with water circulating was added to the simulation, with some of the water going to the solvent stream to replace water lost out the top of the absorber and in the CO2 product

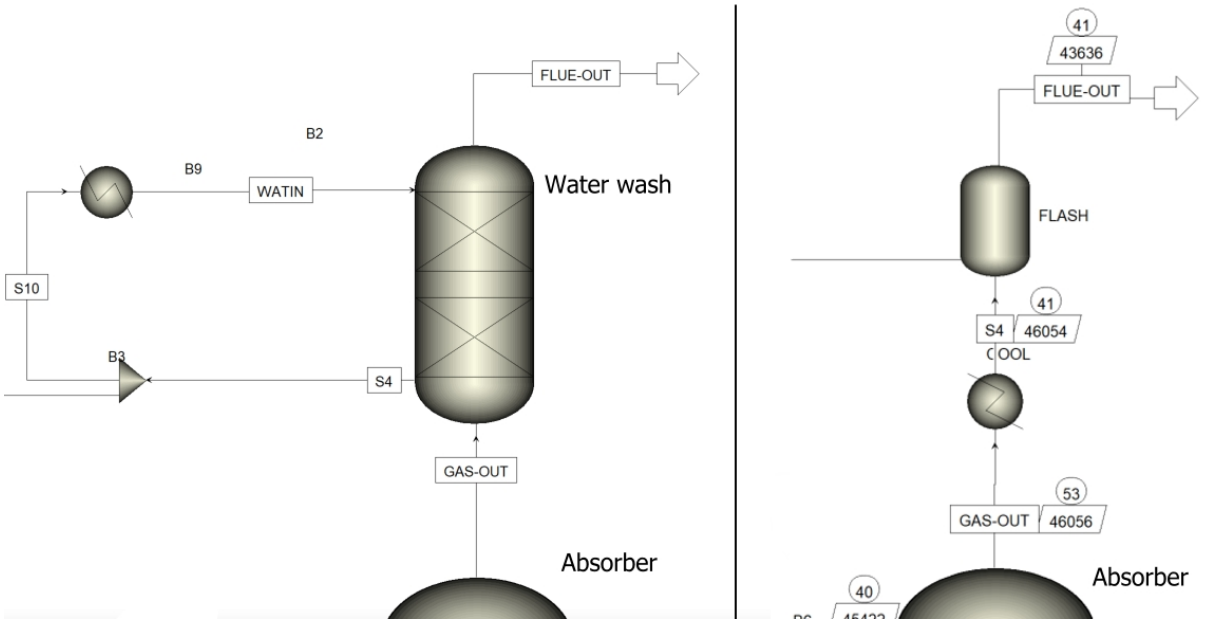

Figure A.4: Caption

stream. This system was difficult to converge, and would be time consuming to converge for all cases, and different solution was used. The water wash was simulated by sending the gas from the absorber to a cooler, cooling the gas to 41 °C, which is 1°C hotter than the flue inlet stream. The cooled gas was then sent into a flash tank to separate the condensate and vapour. The condensate was sent back to the circulating solvent, and the gas was sent out as flue gas. This design had the advantage of being very stable, and sending most of the water and MEA back to the system. The downsides would be that both the amount of water circulating in the water wash and the amount of fresh water used for the system would be unknown and have to estimated. The two configurations are shown in figure A.4.

A.3 Stripper condenser reflux rerouting

Originally the stripper was modeled with a traditional condenser setup. Where the gas coming out the top of the stripper would be cooled to 25 °C in a condenser, and the liquid would be sent back in the stripper. This setup however made the stripper unstable, and a solution to send the condensing liquid directly to the solvent going in to the absorber was tried, and this solution proved much more stable. the liquid coming from the condender were in all cases higher than 99.5 % water. This convergence issue may not have been present if the condenser was modeled inside the radfrac, but the temperatures inside the stripper were lower throught the entire top part. This resulted in a significantly higher reboiler duty. The compared temperature profiles are shown in figure A.5.

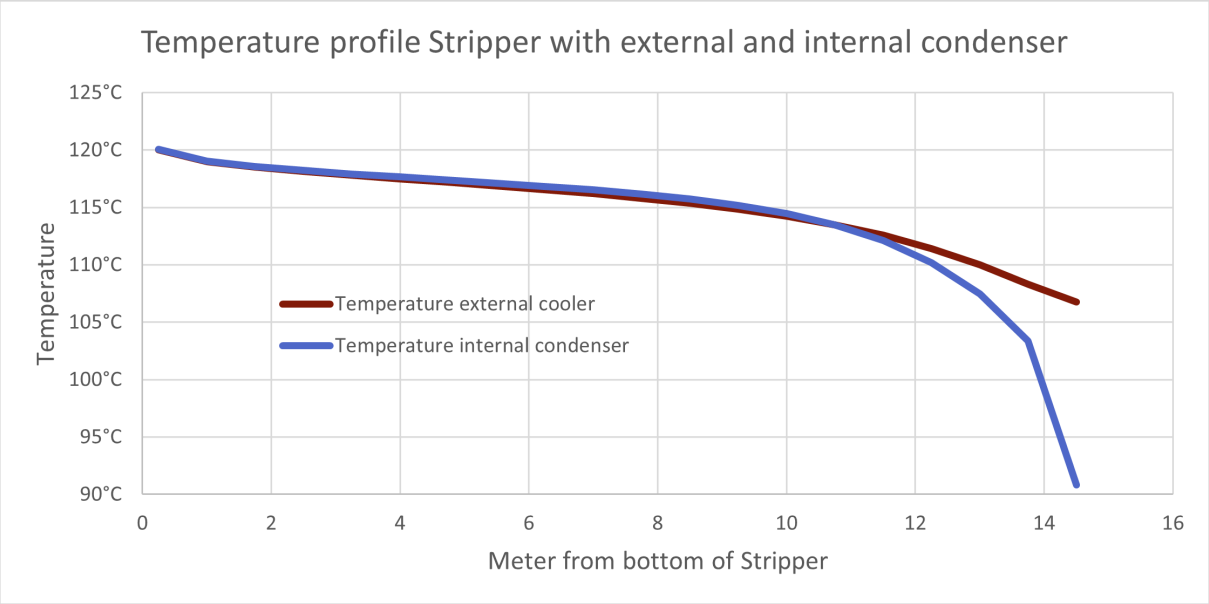

Figure A.5: Caption

A.4 CO_2 capture specification

There are several ways to specify the capture rate of CO_2 in Aspen plus outside of manually tweaking solvent flows and reboiler duties, and several options were tried in this thesis work. The first option implemented was using a design spec block, which specified the gas out stream from the absorber to contain 10% of the CO_2 amount that the inlet gas stream contained. The manipulated variable was the reboiler duty, which would increase or decrease the loading of the lean solvent to achieve the correct capture rate. This system had the benefit of getting precisely 90% capture rate of the CO_2. However, this design resulted in a high number of iterations to converge the flow sheet, and was not very robust. The high number of iterations were due to the solver not getting the response to the change of duty before the absorber had converged with the new duty. In order to address this problem, the design block was changed to specify the CO_2 product stream coming from the condenser on the stripper. This had some of the same problems as the prior design, as the solver did not get the response until after the stripper was converged and the condenser outlet streams were converged. The final solution was to specify the gas stream inside the stripper using design specification in the stripper specifications. The gas outlet stream molar flow of CO_2 would be equal to flue Gas stream CO_2 mole * 0.90. This allowed to the Solver to converge the stripper with the change in duty and capture rate in one go, instead of waiting for other blocks to converge to know the response. This design was very robust when the system was close to a solution or the reboiler duty was too high, ie. too much CO_2 was captured, but would diverge if reboiler duty was much lower than the necessary duty for 90 % capture. To solve this another specification would be used in the stripper if the system was not close to a solution. The temperature in

the bottom stage, the reboiler was specified to 120 °C. When the reboiler temperate was 120°C, the capture rate would not be very far off.